# PIXUL: Developing a High-Throughput Brain Single Nuclei Isolation Protocol for Gene Sequencing Applications

Sabrina Gim

A thesis

submitted in partial fulfillment of the

requirements for the degree of

Master of Science

University of Washington

2025

Committee:

Karol Bomsztyk

Suman Jayadev

Ying Zheng

Program Authorized to Offer Degree:

Bioengineering

University of Washington

**Abstract**

# PIXUL: Developing a High-Throughput Brain Single Nuclei Isolation Protocol for Gene Sequencing Applications

Sabrina Gim
Chair of the Supervisory Committee:
Karol Bomsztyk
Department of Medicine, Pharmacology, and Bioengineering

**Background**
For improved gene sequencing efficiency, in particular snRNA-seq, there's a growing need to develop a protocol capable of isolating nuclei from multiple biological tissue samples at a high-throughput rate while maintaining cost efficiency. Traditional, manual single-nuclei isolation protocols require tissue samples to be individually homogenized using a Dounce homogenizer or a pestle, which limits the number of biological samples that can be processed in a single isolation run. The PIXUL multi-sample megasonicator offers a potential alternative approach to manual homogenization by using ultrasound sonication to automate the homogenization of up to 96 tissue samples in a single isolation cycle.
**Methods**
This project investigates the potential implementation of the PIXUL to homogenize multiple brain tissue samples and generate enough nuclei for gene sequencing applications at a cost-efficient, consistent, high-throughput rate. To test its capabilities of consistently homogenizing multiple brain tissue samples, a single-nuclei isolation protocol integrating the PIXUL was designed, tested, and refined based on preliminary experimental results. Tissue lysis and nuclei quality were assessed using trypan blue staining and microscope imaging. Resulting nuclei concentrations were calculated using a manual hemocytometer counting chamber.
**Results**
The protocol yielded nuclei concentrations between $9.35 \times 10^5$ and $2.01 \times 10^6$ nuclei/mL, which is a comparable range achieved by other manual and automated single nuclei isolation protocols. However, a significant amount of cellular and nuclei debris was observed in all replicates after samples were homogenized. The presence of this debris is likely due to extended sample suspension in lysis buffer, as well as the presence of myelin. This debris may interfere with high-throughput gene sequencing applications.
**Conclusions**
Although this protocol was able to achieve nuclei concentration values that were comparable to other isolation methods for all of its replicates, further experiments focusing on optimizing the PIXUL's setting, finding a method to removal myelin and extracellular DNA, and count nuclei at a high-throughput rate are necessary to improving the reproducibility and efficiency of this novel, high-throughput brain single nuclei isolation protocol.

# Introduction:

Research conducted in the Bomsztyk lab primarily focuses on epigenetic analysis of various debilitating medical conditions and cancers. The medical motivation for this project is primarily focused on central nervous system diseases such as Alzheimer's disease, Parkinson's disease, and glioblastoma. Alzheimer's disease is a progressive, cognitive neurodegenerative disorder that leads to significant memory loss and increased difficulty with familiar tasks. [1] This disease is characterized by the accumulation of amyloid plaques and tau tangles, as well as the widespread dysfunction and death of neurons in the brain. [2] Alzheimer's disease is the 7th leading cause of death in the United States, and there are over 7 million cases of the disease in the United States. [1, 3] Despite these data, the cause of Alzheimer's is still not well understood.

Parkinson's disease is also a progressive neurodegenerative disease that is characterized by tremors, bradykinesia, and the deterioration of dopamine-producing neurons in the brain. [4, 5] It is the 2nd most common neurodegenerative disorder, right behind Alzheimer's disease, and there are approximately 1 million cases in the United States. The incidence of Parkinson's disease is higher in men than women, and the disease typically manifests in patients who are around 60 years old. [6] Similarly to Alzheimer's disease, the cause of Parkinson's disease is not well known.

Glioblastoma (GBM) is the most aggressive and malignant brain cancer across the globe. [7] Although there are only 3.1 cases of GBM diagnosed annually out of every 100,000 cases, GBM accounts for nearly 45.6% of malignant brain tumor cases worldwide. Cases of GBM typically occur in patients who are 64 years old or older, but there have been several cases of childhood GBM documented. [8] Following diagnosis, the prognosis for GBM patients is very poor. Very few patients will survive 2.5 years post-diagnosis, and fewer than 5 % of GBM patients will survive 5 years and beyond. [9] GBM is particularly difficult to treat because it's often resistant to traditional methods of cancer treatment, such as radiotherapy and oral chemotherapy drugs, such as temozolomide, and GBM generally recurs post-treatment. [10] The exact cause of Glioblastoma remains incompletely understood.

In recent years, researchers have been actively using single-nucleus RNA-sequencing (snRNA-seq) to better understand the mechanisms and profiles of these diseases. With snRNA-seq, researchers were able to identify several genes that were positively associated with Alzheimer's disease, specifically the genes involved in mRNA metabolic processing, synaptic signaling, and chromatin organization. [11] Additionally, researchers using snRNA-seq were able to identify a population of somatostatin inhibitory neuron subtypes that were noticeably depleted in Alzheimer's disease brain samples. In a separate study, researchers using snRNA-seq were able to identify 20 differentially expressed genes in dopaminergic neurons in Parkinson's samples, and they also identified several TH-enriched glial subpopulations, such as microglia, astrocytes, and oligodendrocytes, that were noticeably depleted in the Parkinson's samples. [12] For GBM, a number of findings have been made using snRNA-seq. Specifically, snRNA-seq was used to discover that recurrent GBM is associated with a notable cell phenotype shift where the phenotype of proliferating glioblastoma cells will shift from the Verhakk proneural phenotype to the mesenchymal phenotype. Furthermore, these researchers were able to identify specific genes that are expressed in mesenchymal cells when they re-enter the cell cycle. By targeting these

genes, the viability of GBM cells significantly decreases. Additionally, researchers have made significant progress in GBM therapy discovery by using snRNA-seq and successfully developing reliable preclinical models that mirror the most common subtype of human GBM (TMEMed Glioblastoma). This is crucial as human GBM has a heterogeneous tumor microenvironment (TME). The reliability of these preclinical models is important, as the specific TME of the GBM affects treatment response and disease progression. [13] These researchers confirmed the reliability of their preclinical models using snRNA-seq, which identified key tumor cell states and heterogeneity in the preclinical models that were similarly observed in human GBM stem cells.

Despite these recent discoveries, understanding the complete etiology and signaling progression pathways in patients with Alzheimer's disease, Parkinson's disease, or GBM remains largely a mystery. Therefore, progress towards finding novel methods to improve gene sequencing is imperative for the discovery of reliable therapies and to improve our understanding of the pathogenesis of these diseases. To use gene sequencing applications such as snRNA-seq, nuclei need to first be isolated using a single-nucleus isolation procedure. By designing a high-throughput brain single-nuclei isolation protocol, gene sequencing applications, such as snRNA-seq, can be further optimized to process more genetic samples at a more efficient, higher-throughput rate.

*Existing Single-Nuclei Isolation Methods*

Current single-nuclei isolation methods can be divided into three different categories: manual isolation, nuclei isolation kits, and semi-automated nuclei isolation. Manual isolation protocols involve manual, mechanical lysis of tissue samples using either a Dounce homogenizer, a pestle, or a centrifuge. [14, 15] One notable advantage of manual single nuclei isolation is that it offers more user control and protocol customization, allowing for easier protocol optimization for specialized samples or other experimental needs. The number of samples processed during one isolation run is variable, but it's uncommon to process more than 10 samples at once. Such protocols can produce anywhere between 700 – 1,200 nuclei/μL or $7.0 \times 10^5$ – $1.2 \times 10^6$ nuclei/mL, which is the optimal nuclei concentration for single-nuclei sequencing. Conversely, manual single-nuclei isolation is accompanied by several disadvantages. It's labor-intensive, has a lower throughput, and can lead to variable results based on user technique and experience. Additionally, these protocols are very time-consuming and can take anywhere between 1-3 hours to complete. [16]

In contrast, nuclei isolation kits offered by companies, such as 10x Genomics and Invent Biotechnologies, mitigate some of these limitations by providing pre-formulated buffers and standard protocols. [17, 18] Using pre-formulated buffers and standard protocols allows users to produce standardized, reproducible results in a time-efficient manner, with isolation runs taking 30 minutes to two hours to complete, and these kits can produce up to 1 million nuclei/10 mg or $1.04 \times 10^8$ nuclei/mL using mouse brain samples. Similarly to manual nuclei isolation protocols, the number of samples processed during an isolation run is variable, but it's uncommon to process more than 10 samples at once. Nuclei isolation kits have a few limitations. Most notably, they are more expensive than traditional, manual protocols, with each kit costing approximately

$500, and these kits offer users less flexibility for protocol optimization, as each kit is often designed for a specific model organism and tissue type.

The last method of single-nuclei isolation is the semi-automated isolation method. Semi-automated single nuclei isolation involves using a specialized device that automates the homogenization of samples through mechanical or chemical methods, or a combination of both. [19, 20] Similar to the nuclei isolation kits, the companies producing semi-automated machines, such as Miltenyi Biotec and S2 genomics, offer users the option to use their pre-formulated buffers and enzymes to minimize preparation time and reduce variability in results, but users have the option of using lab-prepared buffers with these devices. Semi-automated single nuclei isolation methods are able to isolate nuclei at a higher-throughput and reproducible rate in less than 30 minutes using specialized devices such as The Singulator 200 created by S2 genomics. [20] Devices such as The Singulator 100 can consistently produce up to $9.09 \times 10^5$ nuclei/mL using frozen mouse brain tissue for single-nuclei gene sequencing applications. Although these devices can reliably and efficiently isolate nuclei at a high-throughput rate using either pre-formulated or lab-prepared reagents, these devices and their proprietary consumables, such as required cartridges and tubes, can be expensive to purchase over time, and these devices may not be readily accessible to many researchers.

Given the associated advantages and disadvantages of each single-nuclei isolation method, there is a need to develop a more affordable single-nuclei isolation method that achieves the high-throughput efficiency of semi-automated isolation methods, the flexible protocol customization and optimization of manual isolation methods, and the result reproducibility of nuclei isolation kits.

*PIXUL: Multi-Sample Sonicator*

In collaboration with his colleagues, Dr. Bomsztyk and his team developed a novel, multi-sample sonicator device named the PIXUL. [21] In particular, the “U” in the moniker refers to the array of ultrasound transducers used within the PIXUL to shear fresh or frozen tissue samples or other genetic material such as chromatin. The PIXUL is comprised of four main parts: an array of ultrasound transducers that focus ultrasound waves into every well in a 96-well polystyrene (PS) or polypropylene (PP) microplate, an amplifier to power the transducers, a Peltier cooling system to control the temperature of the environment that houses the samples and a computer that controls the entire device based on the following set of variable parameters: Pulse, Pulse-repetition frequency (PRF), Burst, and Time. The pulse parameter describes the number of 2 MHz ultrasound wave cycles per pulse, the PRF parameter describes the delay between pulses in kHz, and the burst rate parameter describes the frequency at which sets of pulses transition to the next, neighboring columns (there are a total of 12 columns). The time parameter describes the process duration of a given run. The default settings of the PIXUL are as follows: Pulse (N) = 50, PRF (kHz) = 1, Burst Rate (Hz) = 20, and Time Duration (min) = 30.

To shear tissue or other genetic material, the PIXUL emits ultrasound waves to create alternating cycles of high and low pressure within each sample. The lower pressure enables gas bubble formation within the fluid, and the higher pressure leads to the sudden collapse of the

bubbles, generating enough hydrodynamic shear stress to shear samples. The novelty of the PIXUL lies in its ability to simultaneously process up to 96 separate samples in traditional 96-well microplates. The PIXUL's ability to directly transmit ultrasound waves into each well in a 96-well microplate is particularly innovative because other commercially available semi-automated single nuclei isolation devices cannot process samples housed inside 96-well microplates. If users use a 96-well microplate to hold their samples, they will need to transfer their samples from the microplate to individual, compatible tubes, which is an inefficient process that could lead to significant sample loss. Additionally, these competing devices can only simultaneously process a limited number of samples. For instance, semi-automated single nuclei isolation devices such as The Singulator 200 and the gentleMACS Octo Dissociator can only process up to two and eight samples at once, respectively. [19, 20] Furthermore, the proprietary consumable tubes used for these devices are often costly. For instance, the M tubes used for the gentleMACS Octo Dissociator cost approximately $205 for a set of 25 sterile tubes. In direct contrast, the PIXUL uses 96-well microplates that are approximately $2 per plate, and unlike the gentleMACS Octo Dissociator and The Singulator 200, the PIXUL can process up to 96 samples during a single sonication run. The PIXUL's ability to process a high number of samples in a low-cost 96-well microplate makes it an appealing device choice for the development of a more cost-effective, high-throughput single-nuclei isolation protocol. However, it's important to acknowledge a few potential concerns regarding the use of the PIXUL. In particular, there are environmental concerns regarding the use of 96-well microplates, as polypropylene is not biodegradable, and the disposal of these 96-well microplates continues to contribute to landfills across the globe. [22] Additionally, although these 96-well microplates are much more affordable compared to the proprietary tubes used by other commercially available competitor devices, the PIXUL device itself can be a major financial investment, and maintenance can drive up the overall cost of using the PIXUL. [21] However, given all of these considerations, the PIXUL has significant potential to process up to 96 samples at a more affordable cost and higher-throughput rate than other semi-automated single nuclei isolation devices, and, similar to manual single nuclei isolation methods, the PIXUL can offer users similar protocol flexibility in terms of protocol optimization and customization. Moreover, the PIXUL's ability to reliably emit uniform sonication waves across the entire 96-well microplate suggests that it can potentially achieve similar reproducibility rates as commercially available nuclei isolation kits.

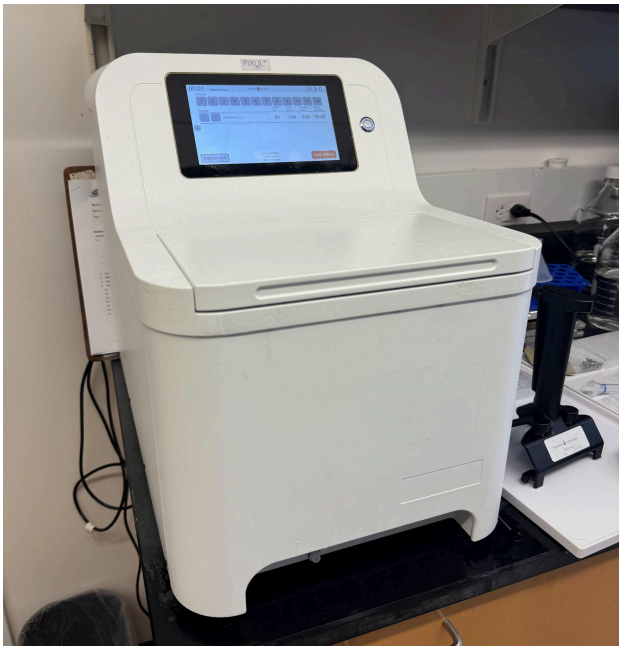

Fig 1. PIXUL Multi-Sample Sonicator. A tissue and genetic material shearing device developed and produced by the Bomsztyk lab and Matchstick Technologies. Up to 96 samples in a 96-well microplate can be simultaneously processed in the PIXUL.

Manual single nuclei isolation protocols rely on require users to manually homogenize their tissue samples using a Dounce homogenizer, a pestle, or through centrifugation methods, which is a labor-intensive and time-consuming process that limits the number of samples that can be processed in a single isolation run. [14, 15] Consequently, these manual protocols yield fewer nuclei compared to semi-automated single-nuclei isolation methods. The PIXUL offers a promising solution to this limitation by efficiently and evenly shearing up to 96 tissue and genetic samples in a 96-well microplate using ultrasound sonication. By using a high-throughput shearing device, such as the PIXUL, to automate the homogenization of tissue samples, the homogenization process for single nuclei isolation can become more streamlined and time-efficient, and a large nuclei yield can be achieved.

A 2022 project in the Bomsztyk lab previously investigated the PIXUL's potential to efficiently homogenize mouse liver tissue for high-throughput single nuclei isolation. [23] After making strategic adjustments to the buffer ratios in the lysis and nuclei wash buffers and increasing the number of wash steps, the final nuclei yield was able to reach up to 5,000 nuclei/µL, which is comparable to other manual nuclei isolation protocols, however, the final nuclei yield of these experiments often varied and many experiments resulted in unsatisfactory nuclei yields. Additionally, the entire protocol takes 3.5 hours to complete, which leaves room for improvement in overall protocol efficiency.

This thesis aims to build upon this previous protocol to develop a high-throughput, efficient single-nuclei isolation protocol that leverages PIXUL's ability to homogenize frozen mouse brain tissue. Frozen mouse brain tissue samples were chosen for their relevance to epigenetic research focused on the etiology and treatment of different central nervous system

diseases. To optimize and improve the previous protocol to homogenize frozen mouse brain tissue, several preliminary experiments were performed to optimize the lysis buffer, PIXUL's settings, and the number of frozen tissue cores used for each sample.

# Development of Design Specifications:

*Trypan Blue Dye: Nuclei Staining*

Trypan blue is a negatively charged dye that is traditionally used to differentiate between live and dead cells in a suspension. This staining method works by mixing trypan blue dye in a 1:1 ratio with a cell suspension, and this dye will stain the cytoplasm and nuclei of dead cells dark blue. Because live cells have intact, lipid-based cell membranes, trypan blue dye cannot penetrate through the membrane and stain the inner cell contents. As a result, live cells will remain visibly clear or pale after trypan blue dye is mixed in with a sample suspension. In addition to differentiating between live and dead cells, trypan blue dye also acts as a useful staining tool to observe and count intact nuclei under a microscope and assess the extent of cell lysis after brain tissue samples are homogenized in a lysis buffer. After each sample was placed in lysis buffer and homogenized using the PIXUL, trypan blue staining was performed to assess the lysis efficiency and quality of nuclei.

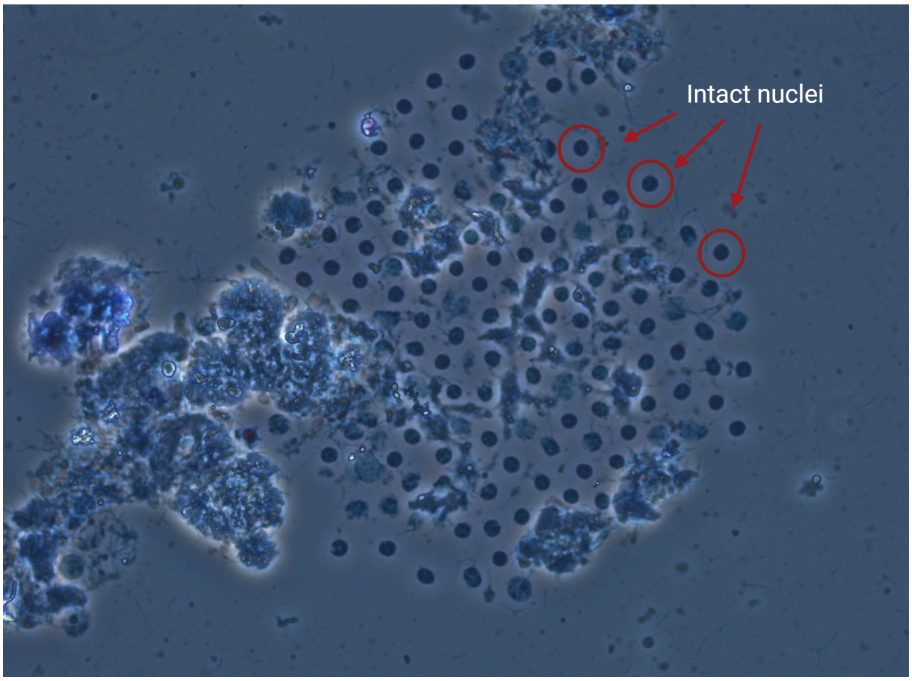


Fig 2. Trypan blue staining of mouse brain nuclei right after tissue homogenization and cell lysis.

*Hemocytometer: Manual Counter for Nuclei*

To determine the final nuclei concentration of the suspensions produced, a manual cell counter called a hemocytometer was used. A manual cell counter was chosen over an automated cell counter due to the excessive amounts of cellular debris produced by brain tissue samples, which can interfere with the automated cell counter's ability to accurately count the intact brain nuclei. There are a few limitations with using a hemocytometer to count nuclei; notably, these devices often cause excessive eye strain and fatigue, which can contribute to counting errors. Additionally, it's important to acknowledge that using a manual cell counter is not suitable for counting nuclei for high-throughput applications, but for the purposes of maintaining accuracy, especially during the protocol development phase, we decided to use a manual cell counter to accurately calculate the final nuclei concentration values.


Fig 3. Hemocytometer and hand-held tally counter used in the Bomsztyk lab.

*CryoCore: Extracting Frozen Brain Tissues Cores*

The CryoCore system consists of a hand-held rotary tool, a CryoTray, a CryoBlock, and a CryoBox. The CryoTray holds all of the mouse brain samples prior to extraction, and the CryoBox is a styrofoam box filled with dry ice. The CryoBlock, which is placed inside the CryoBox, is used to provide a stable foundation for the CryoTray during extraction, and it's used to keep samples below a temperature of -70℃. By loading the CryoCore with PBS solution and using the hand-held rotary tool, 1-2mm$^3$ tissue cores can be extracted, and each core contains around 1-2 mg of tissue.

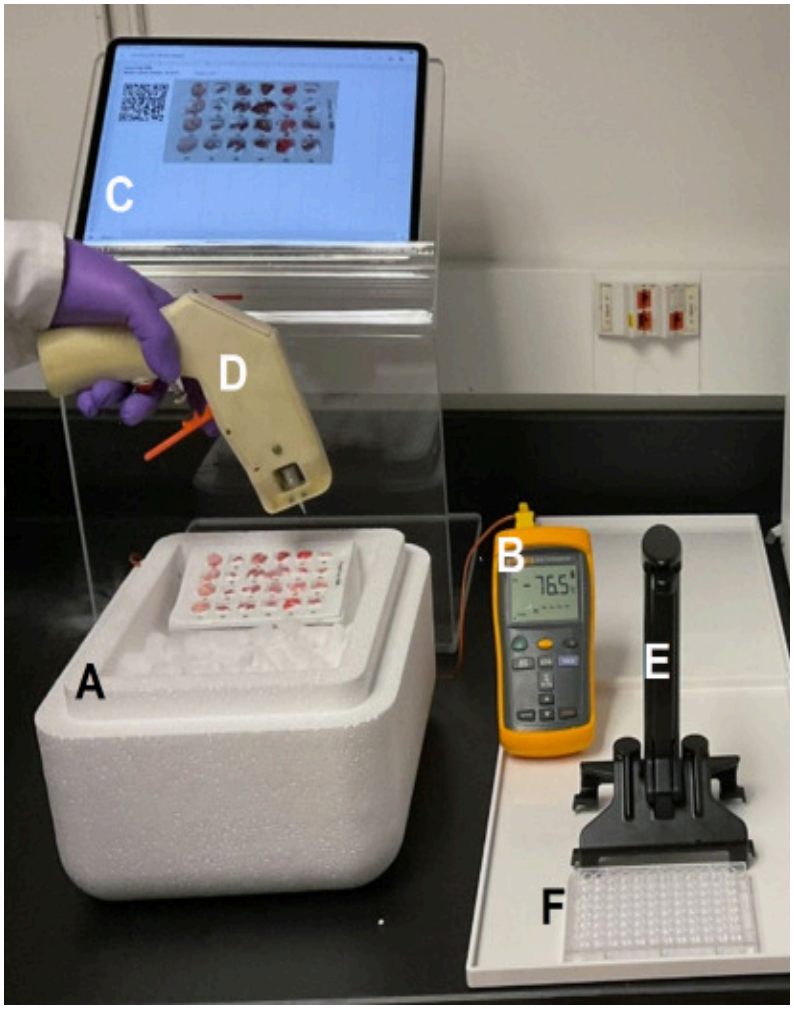


Fig 4. CryoCore: a hand-held rotary extraction tool that produces 1-2mm$^3$ brain tissue cores, which contain around 1-2 mg of brain tissue. The CryoBox is filled with dry ice and holds both the CryoBlock and CryoTray. [23]

*Centrifuge: Separate Nuclei from Cellular Debris*

To properly separate the nuclei from other cellular debris in the suspension, it's important to perform several wash steps by first spinning the nuclei suspension down using a centrifuge. The centrifuge used in the Bomsztyk lab uses micro test tubes, which range in size from 0.2 mL to 2 mL. For all of the experiments performed, nuclei suspensions were spun at 500 g for 5 minutes at 4℃. It was important that samples were centrifuged down at 4℃ to inhibit additional enzymatic lysis activity as well as maintain the integrity of the nuclei. Once done processing in the centrifuge, a nuclei pellet was observed at the bottom of each test tube.


Fig 5. Centrifuge used in the Bomsztyk lab.

*Cell Strainers: Filter Nuclei from Tissue and Cellular Debris*

To filter the nuclei and separate the nuclei from tissue and cellular debris, three different-sized cell strainers were used: a 200 µm cell strainer, a 70 µm cell strainer, and a 40 µm cell strainer. The 200 µm cell strainer was used to remove large brain tissue aggregates from the sample suspension, and the 70 µm cell strainer was used to remove smaller brain tissue aggregates from the sample suspension. The 40 µm cell strainer was used to properly filter the neuronal nuclei, which are approximately 8-10 µm in diameter on average. [24]


Fig 6. Cellstrainers (40 µm, 70 µm, and 200 µm) used in the Bomsztyk lab.

*96-well Plate Shaker*

In an attempt to promote the lysis of brain cells and minimize nuclei and cell aggregation, a 96-well plate shaker was used right after the homogenization of samples at the following settings: 3 minutes at 300 rpm. When samples were observed under a microscope with trypan blue staining, most of the nuclei were ruptured. The plate shaker settings were then adjusted to the following settings: 1 minute at 300 rpm; however, similar results were observed. The plate shaker settings were then adjusted to 30 seconds at 300 rpm with similar results.


Fig 7. 96-well plate shaker.

However, when brain tissues samples were homogenized in the PIXUL at the following settings: Pulse (N): 20, PRF (kHz): 1, Burst Rate (Hz): 50, and Time Duration (min): 4, and then transferred to the 96-well plate shaker for 15 seconds at 300 rpm, there was no observable improvements in nuclei yield or cell and nuclei aggregation. Given these findings, the plate shaker was ultimately omitted in the final single-nuclei isolation protocol.

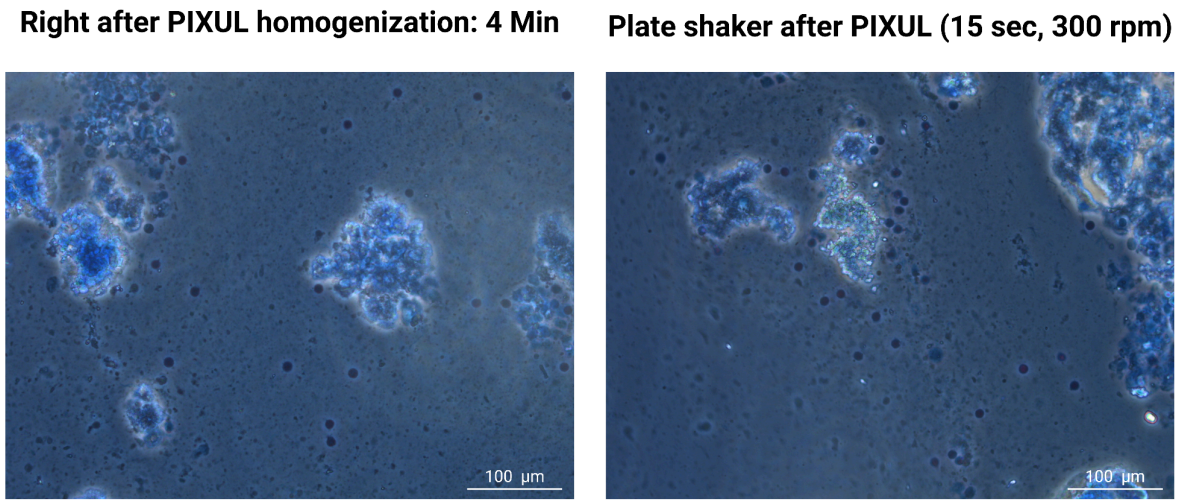


Fig 8. Trypan blue staining of a brain tissue sample (10 tissue cores) was performed right after tissue homogenization, and after plate was put on a plate shaker after homogenization. Scale bar is 100 µm.

**Preliminary Experiment 1:** *Optimizing the Lysis Buffer Recipes*

To achieve a high nuclei yield, it's important to choose an appropriate lysis buffer that adequately lyses the cells without degrading the nuclei. Additionally, the lysis buffer must create a stable pH and osmotic environment to prevent nuclei from aggregating or being completely degraded. To create the most optimized lysis buffer, it was important to design an experiment that would directly assess the lysis efficiency of each lysis buffer. Briefly, an experiment was conducted using two identical brain tissue samples, which were then homogenized in the PIXUL with the following settings: Pulse (N): 20, PRF (kHz): 1, Burst Rate (Hz): 50, and Time Duration (min): 4. These samples were then filtered through a 70 µm and a 40 µm cell strainer, and their post-filtration nuclei yield was examined using trypan blue staining.

Three different lysis buffers were tested using the same experimental protocol mentioned briefly above. The first lysis buffer assessed was the same lysis buffer used in the 2022 Bomsztyk liver single nuclei isolation protocol. This buffer contained the following reagents: 1 M Tris-HCl (pH 7.4), 5 M NaCl, 1 M $MgCl_2$, and the lysis reagent with 10 % HEPES/$HgCl_2$/KCl/NP.40/nuclease-free $H_2O$. The Tri-HCl buffer was used to create a stable pH environment for the nuclei, and the salts, NaCl and $MgCl_2$, were used to create a stable osmotic environment for the nuclei. Finally, the lysis reagent with 10 % HEPES/$HgCl_2$/KCl/NP.40/nuclease-free $H_2O$ was used to lyse the cells and release the nuclei. Additionally, the nuclei wash buffer from the 2022 Bomsztyk liver single nuclei isolation protocol was used in the same experiment. This nuclei wash buffer consists of the following reagents: 5% BSA, 40U/µL RNase inhibitor, and 1X PBS. The 5% BSA was used to prevent the

aggregation of nuclei, and the RNase inhibitor was used to inhibit additional enzymatic lysis of cells and nuclei.

The second lysis buffer tested was a lysis buffer that's very similar to the lysis buffer used in the Jayadev lab. This lysis buffer has been used to successfully isolate nuclei in the Jayadev lab. This lysis buffer consists of the following reagents: nuclei wash buffer, 10% BSA, 1 mM ATA, 10% NP-40, 10% Tween-20, and 5% digitonin. The 10% BSA was used to limit the amount of nuclei aggregation, and the 1 mM ATA was used to prevent the enzymatic degradation of intact nuclei. The 10% NP-40, 10% Tween-20, and 5% digitonin were used to enhance the lysis of cells and the release of nuclei. Additionally, the nuclei wash buffer used in the Jayadev lab nuclei isolation protocols was also tested in the same experiment. This nuclei wash buffer consists of 10% BSA, 40 U/μL protein RNase inhibitor, and 1X PBS. Similar to the nuclei wash buffer used in the 2022 Bomsztyk liver single nuclei isolation protocol, the 10% BSA used in this recipe is used to limit nuclei aggregation, and the protein RNase inhibitor is used to inhibit additional enzymatic lysis activity.

The last lysis buffer tested was an optimized lysis buffer that takes different components from the two previously mentioned lysis buffers. This lysis buffer consists of the following reagents: 10% NP-40, 10% BSA, 1 M Tris-HCl (pH 7.4), $MgCl_2$, NaCl, 5% digitonin, and nuclease-free water. The 10% NP-20 and 5% digitonin were used to enhance the lysis of cells and release of nuclei, and the 10% BSA was used to reduce nuclei aggregation. The Tri-HCl buffer was used to create a stable pH environment for the nuclei, and the salts, NaCl and $MgCl_2$, were used to create a stable osmotic environment for the nuclei. To test this lysis buffer with the experimental protocol briefly mentioned above, the same Jayadev lab nuclei wash buffer was used.

**Preliminary Experiment 2:** *Optimizing the Number of Tissue Cores for each Sample*

To maximize the nuclei yield, it was important to consider how much frozen mouse brain tissue would be extracted for each sample. If each sample contains an insufficient amount of brain tissue, very few nuclei would be extracted during the lysis process, and subsequent filtering could lead to further reductions in nuclei yield. However, if each sample contains an excessive amount of brain tissue, the processing time in the PIXUL will likely need to be extended to effectively lyse the cells and extract nuclei, which would reduce the overall efficiency of the homogenization process. To investigate this, an experiment was conducted using 5 brain tissue samples, with each sample having the following number of frozen mouse brain tissue cores: 2, 4, 6, 8, and 10 cores. These samples were then processed in the PIXUL at the following settings: Pulse (N): 20, PRF (kHz): 1, Burst Rate (Hz): 50, and Time Duration (min): 4. These samples were then filtered through a 200 μm cell strainer, and their post-filtration nuclei yields were examined using trypan blue staining.

**Preliminary Experiment 3:** *Optimizing the PIXUL Settings*

Given how delicate brain tissue is compared to other tissue types, it was important to make appropriate adjustments to the PIXUL settings so that the frozen mouse brain tissue is homogenized thoroughly without damaging the nuclei. To reduce the amount of focused

ultrasound energy to each sample, the Pulse setting was decreased to 20 cycles per pulse, and the Burst Rate was increased to 50 Hz to minimize the transition delays of ultrasound pulses between columns. This helps ensure samples in different columns are evenly and equally homogenized.

To make the most optimal settings adjustments, a preliminary experiment was conducted with five identical brain tissue samples, with each sample having 10 tissue cores. Each sample was processed in the PIXUL with the same Pulse (N), PRF (kHz), and Burst Rate (Hz) settings, which were set to 20, 1, and 50, respectively. The five tissue samples were processed in the PIXUL at different durations. Samples 1, 2, 3, 4, and 5 were processed at the following time durations, respectively: 30 seconds, 1 minute, 2 minutes, 4 minutes, and 6 minutes. After homogenization, the samples were filtered through a 70 μm cell strainer, and their post-filtration nuclei yield was examined using trypan blue staining.

# Materials and Methods:

*Source of Frozen Mouse Brain Tissues*

8-12 week old C57bl/6 female mice were injected intraperitoneally with 200 μL of PBS and euthanized 12 hours later by isoflurane overdose and confirmatory cervical dislocation. Mouse brains were then harvested and frozen.

*Preparing the CryoCore for Extraction*

Before the mouse brains were frozen, a CryoBlock was placed in a CryoBox filled with dry ice to maintain a temperature below -70℃. Then, a 24-well CryoTray was prepared by injecting a small amount of CryoGel cryogenic media into each well. This tray was then placed onto the CryoBlock, and the freshly harvested mouse brains were put on ice before being placed into each tray well. The CryoGel cryogenic media at the bottom of the wells helped promote rapid tissue freezing. Frozen tissues were stored in a freezer at -80℃ prior to sampling.

**<u>Preliminary Experiment 1</u>:** *Optimizing the Lysis Buffer Recipes*

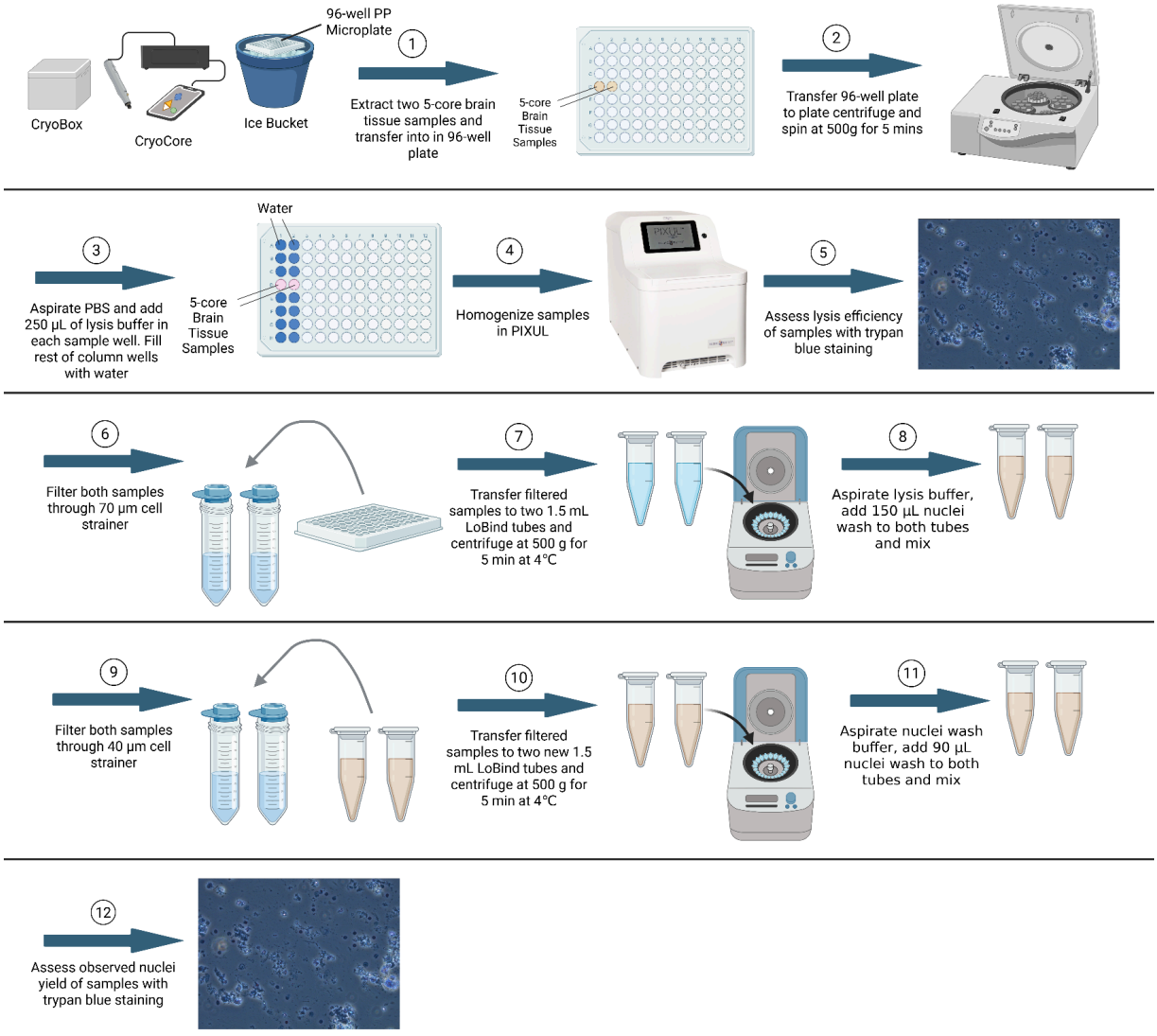


Fig 9. Workflow diagram illustrating the protocol used in the first preliminary experiment [Figure *created in https://BioRender.com*]

*Preparing the Lysis and Nuclei Wash Buffers*

The first preliminary experiment begins by first creating the three lysis buffers and two nuclei wash buffers. The nuclei wash buffer used in the 2022 Bomsztyk liver single nuclei isolation protocol was first made by combining the following reagents: 760 µL of 5% BSA, 19 µL of 40U/µL RNase inhibitor, and 3.021 mL of 1X PBS. Then, the lysis buffer used in the 2022 Bomsztyk liver single nuclei isolation protocol was made by combining the following reagents: 100 µL of 1 M Tris-HCl (pH 7.4), 20 µL of 5 M NaCl, 30 µL of $MgCl_2$, 100 µL of Lysis Reagent (10% HEPES/$HgCl_2$/KCl/NP.40/nuclease-free $H_2O$), and 9.75 mL nuclease-free water.

| 2022 Bomsztyk lab Nuclei Wash & Resuspension Buffer | Stock | Final | Volume |
|---|---|---|---|
| 5% BSA | 5% | 1% | 760 µL |
| RNase inhibitor | 40 U/µL | 0.2 U/µL | 19 µL |
| 1X PBS | - | - | 3.021 mL |
| Total Volume | | | 3.8 mL |

Table 1. Nuclei wash buffer recipe used in the 2022 Bomsztyk lab liver single nuclei isolation protocol.

| 2022 Bomsztyk lab Lysis Buffer Recipe | Stock | Final | Volume |
|---|---|---|---|
| Tris-HCl (pH 7.4) | 1 M | 10 mM | 100 µL |
| NaCl | 5 M | 10 mM | 20 µL |
| $MgCl_2$ | 1 M | 3 mM | 30 µL |
| Lysis Reagent<br><br>[HEPES/$HgCl_2$/KCl/ NP.40/nuclease-free $H_2O$] | 10% | 0.1% | 100 µL |
| Nuclease-free $H_2O$ | - | - | 9.75 mL |
| Total volume | | | 10 mL |

Table 2. Lysis buffer recipe used in the 2022 Bomsztyk lab liver single nuclei isolation protocol.

The nuclei wash buffer used in the Jayadev lab was made by combining the following reagents: 1.790 mL of 1X PBS, 200 µL of 10% BSA, and 10 µL of 40 U/µL protector RNase inhibitor. Then, the second lysis buffer that's nearly identical to the lysis buffer used in the Jayadev lab was made by combining the following reagents: 3.8 mL of 10X nuclei wash buffer, 400 µL of 10% BSA, 400 µL of 1 mM ATA in nuclei wash buffer, 40 µL of 10% NP-40, 40 µL of 10% Tween-20, and 4 µL of 5% digitonin.

| Nuclei Wash & Resuspension Buffer | Stock | Final | Volume |
|---|---|---|---|
| 1X PBS | 1X | 0.895X | 1.790 mL |
| 10% BSA | 10% | 1% | 200 µL |
| Protector RNase Inhibitor | 40 U/µL | 0.2 U/µL | 10 µL |
| Total Volume | | | 2 mL |

Table 3. Jayadev lab nuclei wash buffer recipe used in their single-nuclei isolation protocols.

| Lysis Buffer Recipe | Stock | Final | Volume |
|---|---|---|---|
| Nuclei Buffer | 10X | 7.78X | 3.8 mL |
| 10% BSA | 10X | 1X | 400 µL |
| 1 mM ATA in Nuclei Buffer | 1 mM | 0.1 mM | 400 µL |
| 10% NP-40 | 10% | 0.1% | 40 µL |
| 10% Tween-20 | 10% | 0.1% | 40 µL |
| 5% Digitonin | 5% | 0.005% | 4 µL |
| Total volume | | | 4 mL |

Table 4. Lysis buffer recipe created using the Jayadev lab's lysis buffer recipe as a reference.

The optimized lysis buffer was prepared by combining the following reagents: 7.84 mL of nuclease-free water, 1 mL of 10% NP-40, 1 mL of 10% BSA, 100 µL of 1 M Tris-HCl (pH 7.4), 30 µL of 1 M $MgCl_2$, 20 µL of 5 M NaCl, and 10 µL of 5% digitonin.

| Lysis Buffer Recipe | Stock | Final | Volume |
|---|---|---|---|
| Nuclease-free $H_2O$ | - | - | 7.84 mL |
| 10% NP-40 | 10% | 1% | 1 mL |
| 10% BSA | 10X | 1X | 1 mL |
| Tris-HCl, pH 7.4 | 1 M | 10 mM | 100 µL |
| $MgCl_2$ | 1 M | 3 mM | 30 µL |
| NaCl | 5 M | 10 mM | 20 µL |
| Digitonin | 5% | 0.005% | 10 µL |
| Total volume | | | 10 mL |

Table 5. Optimized lysis buffer recipe used in the final, high-throughput single-nuclei isolation protocol.

*CryoCore Protocol: Extracting Frozen Mouse Brain Tissue Cores*

All three lysis buffers were tested using the same protocol as follows. A 96-well microplate was prepared and placed on ice next to the CryoCore. The CryoBox, containing both the CryoTray and CryoBlock, was then removed from the freezer and placed next to the CryoCore. The CryoCore was then loaded with 1X PBS, and the hand-held rotary tool was used to extract 5 brain tissue cores for each sample. Two identical 5-core samples were extracted and placed in columns 1 and 2 of row D in the 96-well microplate, and a clear, adhesive film was applied on top of the 96-well microplate. The plate was then spun down at 500g for 5 minutes, and the clear, adhesive film was removed to aspirate the PBS solution from each sample. Then, 250 µL of lysis buffer was administered to each brain tissue sample, and each sample was gently mixed by pipetting up and down 10 times. The rest of the wells in columns 1 and 2 were each filled with 250 µL of water. Once all wells were loaded, a new clear, adhesive film was applied on top of the 96-well microplate in preparation for the homogenization step using PIXUL.

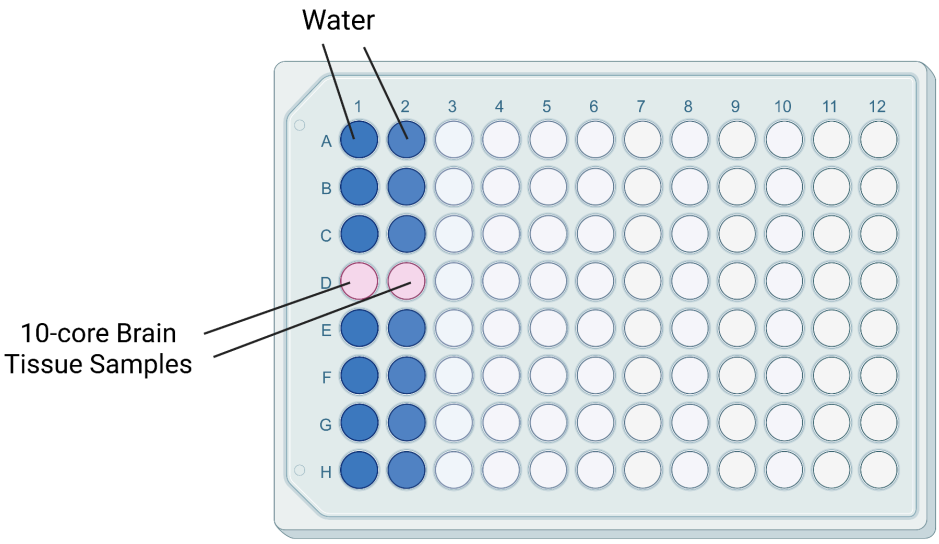


Fig 10. 96-well microplate layout after the two samples are loaded with lysis buffer. [Figure *created in https://BioRender.com*]

*PIXUL Brain Tissue Homogenization Protocol*

The 96-well microplate was carefully loaded into the PIXUL using a hand-held plate holder, and the PIXUL settings were adjusted to the following settings: Pulse (N) = 20, PRF (kHz) = 1, Burst Rate (Hz) = 50, and Time Duration (min) = 4. Once the processing time was completed, the 96-well microplate was removed from the PIXUL, and the plate adhesive film was removed. Each sample was then gently pipetted up and down 10 times to mix the tissue suspension, and the lysis efficiency of each sample was assessed by taking 10 µL of each brain tissue sample suspension and mixing it with 10 µL of trypan blue dye. Then, 10 µL of each mixed solution was deposited onto a glass slide and observed under the microscope.

*Nuclei Filtration Using Cell Strainers Protocol*

Once lysis efficiency was assessed, each sample was carefully removed from the 96-well microplate and individually filtered through a 70 µm cell strainer. Each filtered suspension was transferred to a labeled 1.5 mL LoBind tube and centrifuged at 500g for 5 min at 4℃. Once centrifugation was completed, a pellet was observed at the bottom of each tube, and the lysis buffer above each sample was aspirated.

After the lysis buffer was aspirated, 150 µL of nuclei wash buffer was added to each sample tube, making sure to mix each suspension by pipetting up and down 10 times. Both nuclei suspensions were then filtered through a 40 µm cell strainer, and the filtered suspensions were placed in new 1.5 mL LoBind tubes. These tubes were then centrifuged again at 500g for 5 mins at 4℃, and the supernatant above each pellet was aspirated and replaced with 90 µL of nuclei wash buffer, making sure to pipette each suspension up and down 10 times. The observed nuclei yield was then assessed for each sample by mixing 10 µL of trypan blue dye with 10 µL of

the sample suspension. Then, 10 µL of each mixed solution was deposited onto a glass slide and observed under the microscope.

**<u>Preliminary Experiment 2</u>:** *Optimizing the Number of Tissue Cores for each Sample*

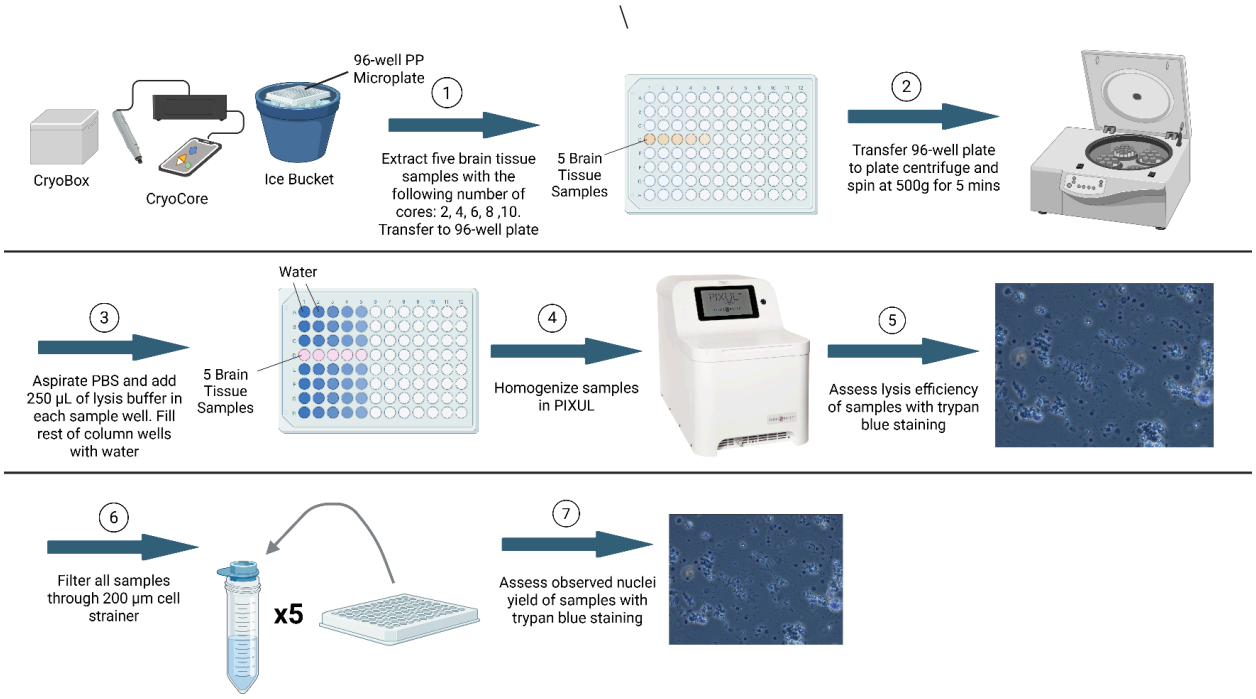


Fig 11. Workflow diagram illustrating the protocol used in the second preliminary experiment [Figure *created in <u>https://BioRender.com</u>*]

*CryoCore Protocol: Extracting Frozen Mouse Brain Tissue Cores*

The second preliminary experiment was conducted using the following protocol. A 96-well microplate was prepared and placed on ice next to the CryoCore. The CryoBox, containing both the CryoTray and CryoBlock, was then removed from the freezer and placed next to the CryoCore. The CryoCore was then loaded with 1X PBS, and the hand-held rotary tool was used to extract 5 brain tissue samples, with each sample having the following number of tissue cores, respectively: 2 cores, 4 cores, 6 cores, 8 cores, and 10 cores. The five brain tissue samples were extracted and placed in columns 1, 2, 3, 4, and 5 of row D in the 96-well microplate, and a clear, adhesive film was applied on top of the 96-well microplate. The plate was then spun down at 500g for 5 minutes, and the clear, adhesive film was removed to aspirate the PBS solution from each sample. Then, 250 µL of the optimized lysis buffer was administered to each brain tissue sample, and each sample was gently mixed by pipetting up and down 10 times. The rest of the wells in columns 1 through 5 were each filled with 250 µL of water. Once all wells were loaded, a new clear, adhesive film was applied on top of the 96-well microplate in preparation for the homogenization step using PIXUL.

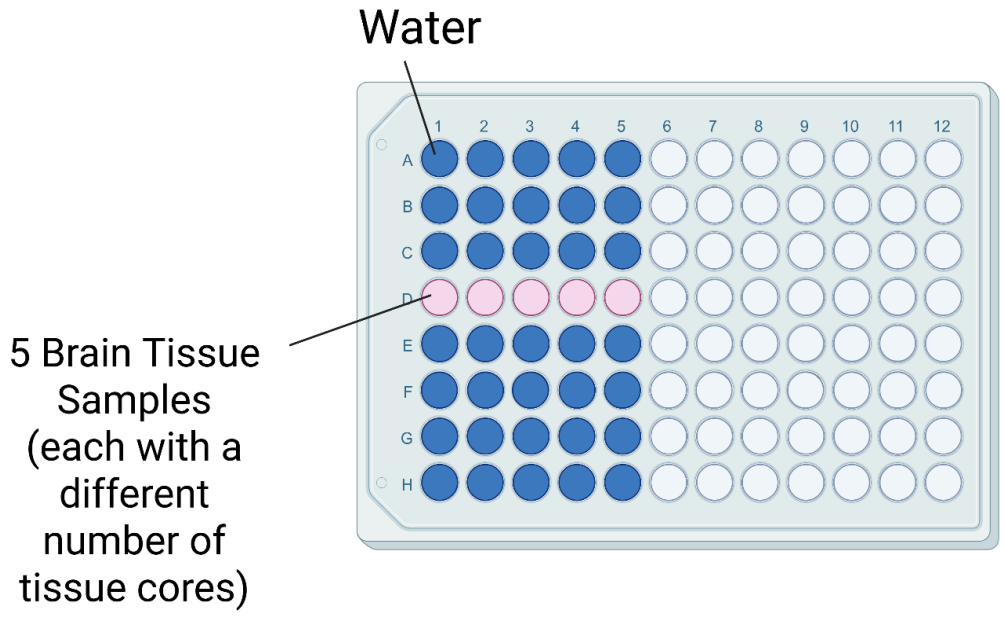


Fig 12. 96-well microplate layout after the five samples (each sample has a different number of tissue cores) are loaded with lysis buffer. [Figure *created in https://BioRender.com*]

*PIXUL Brain Tissue Homogenization Protocol*

The 96-well microplate was carefully loaded into the PIXUL using a hand-held plate holder, and the PIXUL settings were adjusted to the following settings: Pulse (N) = 20, PRF (kHz) = 1, Burst Rate (Hz) = 50, and Time Duration (min) = 4. Once the processing time was completed, the 96-well microplate was removed from the PIXUL, and the plate adhesive film was removed. Each sample was then gently pipetted up and down 10 times to mix the tissue suspension, and the lysis efficiency of each sample was assessed by taking 10 µL of each brain tissue sample suspension and mixing it with 10 µL of trypan blue dye. Then, 10 µL of each mixed solution was deposited onto a glass slide and observed under the microscope.

*Nuclei Filtration Using Cell Strainers Protocol*

Once lysis efficiency was assessed, each samples were carefully removed from the 96-well microplate and individually filtered through a 200 µm cell strainer. Then, the observed nuclei yield was assessed for each sample by mixing 10 µL of trypan blue dye with 10 µL of a sample suspension. Then, 10 µL of each mixed solution was deposited onto a glass slide and observed under the microscope.

**<u>Preliminary Experiment 3</u>:** *Optimizing the PIXUL Settings*

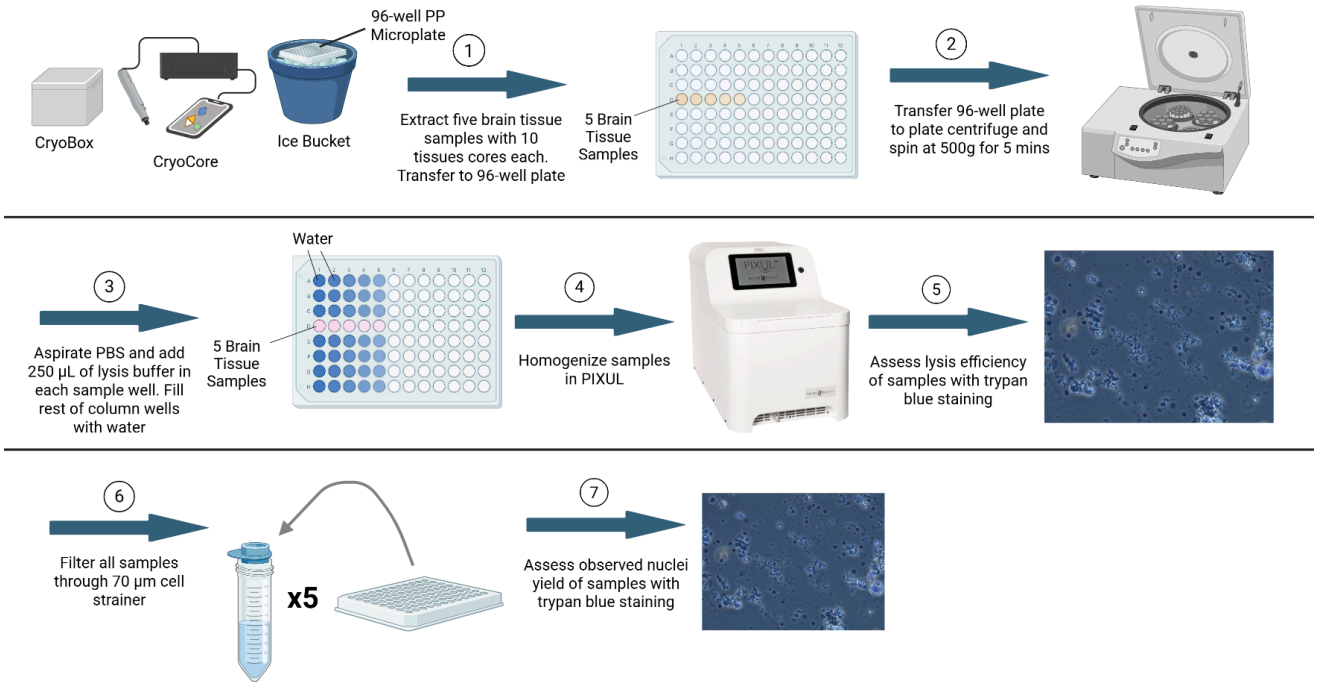


Fig 13. Workflow diagram illustrating the protocol used in the third preliminary experiment [Figure *created in <u>https://BioRender.com</u>*]

*CryoCore Protocol: Extracting Frozen Mouse Brain Tissue Cores*

The third preliminary experiment was conducted using the following protocol. A 96-well microplate was prepared and placed on ice next to the CryoCore. The CryoBox, containing both the CryoTray and CryoBlock, was then removed from the freezer and placed next to the CryoCore. The CryoCore was then loaded with 1X PBS, and the hand-held rotary tool was used to extract 5 identical brain tissue samples, with each sample having 10 tissue cores. The five brain tissue samples were extracted and placed in columns 1, 2, 3, 4, and 5 of row D in the 96-well microplate, and a clear, adhesive film was applied on top of the 96-well microplate. The plate was then spun down at 500g for 5 minutes, and the clear, adhesive film was removed to aspirate the PBS solution from each sample. Then, 250 µL of the optimized lysis buffer was administered to each brain tissue sample, and each sample was gently mixed by pipetting up and down 10 times. The rest of the wells in columns 1 through 5 were each filled with 250 µL of water. Once all wells were loaded, a new clear, adhesive film was applied on top of the 96-well microplate in preparation for the homogenization step using PIXUL.

*PIXUL Brain Tissue Homogenization Protocol*

The 96-well microplate was carefully loaded into the PIXUL using a hand-held plate holder, and all samples had the same Pulse, PRF, and Burst Rate settings. All samples were processed in the PIXUL at the following settings: Pulse (N) = 20, PRF (kHz) = 1, Burst Rate (Hz) = 50, but each sample was homogenized for different durations. Samples 1, 2, 3, 4, and 5 were homogenized for the following durations, respectively: 30 seconds, 1 minute, 2 minutes, 4 minutes, and 6 minutes. Once all samples were homogenized in the PIXUL, the 96-well microplate was removed from the PIXUL, and the plate adhesive film was removed. Each sample was then gently pipetted up and down 10 times to mix the tissue suspension, and the lysis efficiency of each sample was assessed by taking 10 µL of each brain tissue sample suspension and mixing it with 10 µL of trypan blue dye. Then, 10 µL of each mixed solution was deposited onto a glass slide and observed under the microscope.

*Nuclei Filtration Using Cell Strainers Protocol*

Once lysis efficiency was assessed, each samples were carefully removed from the 96-well microplate and individually filtered through a 70 µm cell strainer. Then, the observed nuclei yield was assessed for each sample by mixing 10 µL of trypan blue dye with 10 µL of a sample suspension. Then, 10 µL of each mixed solution was deposited onto a glass slide and observed under the microscope.

## **Finalized Protocol**: PIXUL High-Throughput Brain Single Nuclei Isolation

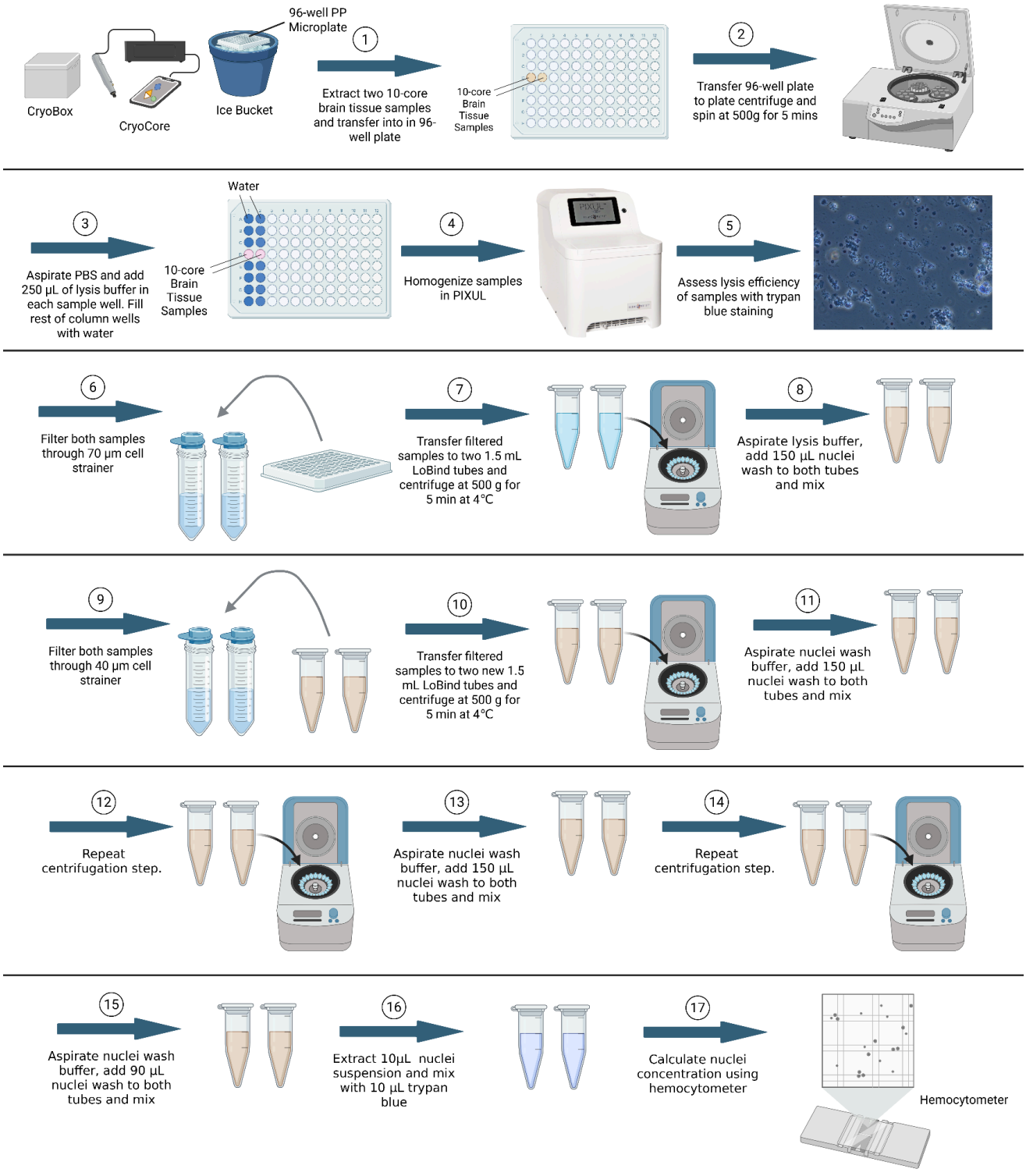


Fig 14. Workflow diagram illustrating the finalized, high-throughput mouse brain single-nuclei isolation protocol using the PIXUL. [Figure *created in https://BioRender.com*]

*CryoCore Protocol: Extracting Frozen Mouse Brain Tissue Cores*

The finalized high-throughput brain single-nuclei isolation protocol is detailed as follows. A 96-well microplate was prepared and placed on ice next to the CryoCore. The CryoBox, containing both the CryoTray and CryoBlock, was then removed from the freezer and placed next to the CryoCore. The CryoCore was then loaded with 1X PBS, and the hand-held rotary tool was used to extract two identical 10 brain tissue-core samples, which were placed in columns 1 and 2 of row D in the 96-well microplate. A clear, adhesive film was then applied on top of the 96-well microplate, and the plate was then spun down at 500g for 5 minutes. The clear, adhesive film was then removed to aspirate the PBS solution from each sample. Then, 250 µL of the optimized lysis buffer was administered to each brain tissue sample, and each sample was gently mixed by pipetting up and down 10 times. The rest of the wells in columns 1 and 2 were each filled with 250 µL of water. Once all wells were loaded, a new clear, adhesive film was applied on top of the 96-well microplate in preparation for the homogenization step using PIXUL.

*PIXUL Brain Tissue Homogenization Protocol*

The 96-well microplate was carefully loaded into the PIXUL using a hand-held plate holder, and the PIXUL settings were adjusted to the following settings: Pulse (N) = 20, PRF (kHz) = 1, Burst Rate (Hz) = 50, and Time Duration (min) = 2. Once the processing time was completed, the 96-well microplate was removed from the PIXUL, and the plate adhesive film was removed. Each sample was then gently pipetted up and down 10 times to mix the tissue suspension, and the lysis efficiency of each sample was assessed by taking 10 µL of each brain tissue sample suspension and mixing it with 10 µL of trypan blue dye. Then, 10 µL of each mixed solution was deposited onto a glass slide and observed under the microscope.

*Nuclei Filtration Using Cell Strainers Protocol*

Once lysis efficiency was assessed, each sample was carefully removed from the 96-well microplate and individually filtered through a 70 µm cell strainer. Each filtered suspension was transferred to a labeled 1.5 mL LoBind tube and centrifuged at 500g for 5 min at 4℃. Once centrifugation was completed, a pellet was observed at the bottom of each tube, and the lysis buffer above each sample was aspirated.

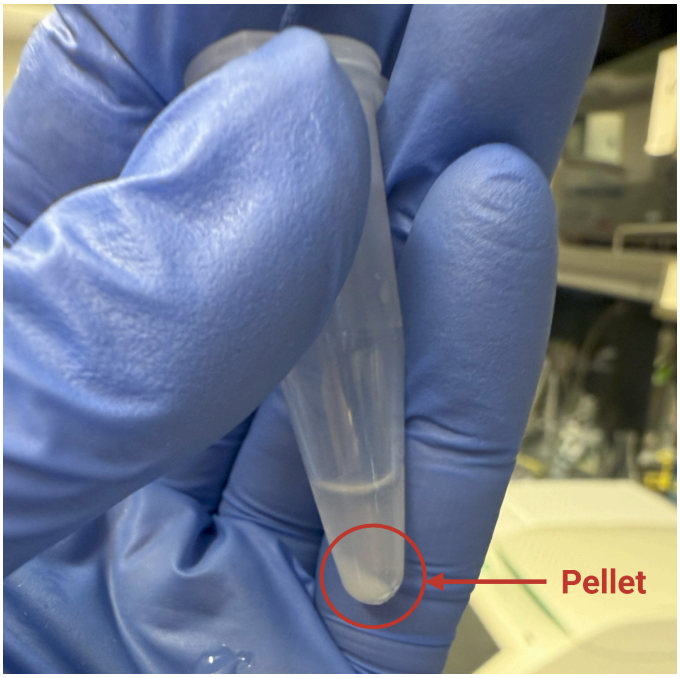


Fig 15. Pellet containing nuclei was observed at the bottom of the sample tubes after centrifugation.

After the lysis buffer was aspirated, 150 µL of nuclei wash buffer was added to each sample tube, making sure to mix each suspension by pipetting up and down 10 times. Both nuclei suspensions were then filtered through a 40 µm cell strainer, and the filtered suspensions were placed in new 1.5 mL LoBind tubes. These tubes were then centrifuged again at 500g for 5 mins at 4℃, and the supernatant above each pellet was aspirated and replaced with 150 µL of nuclei wash buffer, making sure to pipette each suspension up and down 10 times. The two sample tubes were centrifuged again at the same settings, and the supernatants were removed and replaced with 150 µL of nuclei wash buffer again, making sure to pipette each suspension up and down 10 times. The centrifugation and aspiration steps were repeated once more, except that 90 µL of nuclei wash buffer was dispensed to both sample tubes and gently mixed by pipetting up and down 10 times.

*Hemocytometer: Calculating Final Nuclei Concentration*

To calculate the final concentration of the two nuclei suspensions, the hemocytometer chamber surface and the coverslip were first cleaned with 70% ethanol. Then, the coverslip was positioned over the chamber, and, for each sample tube, a 1:1 solution was prepared by mixing 10 µL of the final nuclei suspension with 10 µL of trypan blue by gently pipetting up and down five times. Once prepared, 10 µL of this mixed solution was carefully loaded into the V-shaped well between the chamber and coverslip of the hemocytometer, which was then positioned under the microscope for counting.

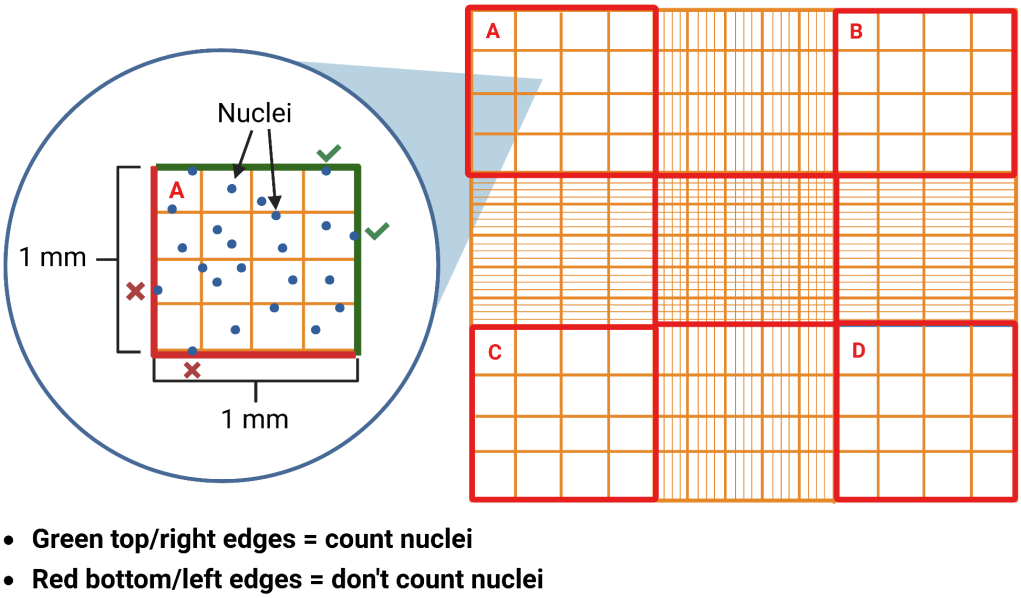


Fig 16. Microscope view of the grid layout of a hemocytometer. Grids A, B, C, and D are the only grids in a hemocytometer used for counting. [Figure *created in https://BioRender.com*]

Once under the microscope, all of the nuclei in grid A of the hemocytometer were counted using a hand-held tally counter, making sure to exclude any nuclei that touched the bottom and left edges of the grid. Once the nuclei count was made, it was multiplied by 2 to account for the dilution by trypan blue dye and was recorded for later calculations. This process was repeated for grids B, C, and D in the hemocytometer, and the final nuclei concentration for each brain tissue sample was calculated using the following formula.

**Total nuclei/mL = 2*([nuclei count in grid A] + [nuclei count in grid B] + [nuclei count in grid C] + [nuclei count in grid D])/4 * $10^4$ [*nuclei/mL]***

# Results:

**Preliminary Experiment 1:** *Optimizing the Lysis Buffer Recipes*

When the lysis and nuclei wash buffers from the 2022 Bomsztyk liver single nuclei isolation protocol were tested against the first preliminary experimental protocol, the nuclei suspension consistently failed to filter through the 40 µm cell strainer. Additionally, when the observed nuclei yields were observed using trypan blue dye, multiple nuclei aggregates were present. One possible explanation for these findings is that the lack of BSA content in the lysis buffer led to the aggregation of the nuclei, which increased the viscosity of the suspension and prevented the suspension from passing through the 40 µm cell strainer. Given these findings, the lysis buffer from the 2022 Bomsztyk liver single nuclei isolation protocol was omitted from both the second and third preliminary experiments, as well as from the finalized single-nuclei isolation protocol.

When the lysis and nuclei wash buffers from the Jayadev lab were tested against the first preliminary experimental protocol, it was apparent that most of the nuclei were predominantly localized near large cellular aggregates, and when these sample suspensions were filtered through both the 70 µm and 40 µm cell strainers, the nuclei yields were significantly lower. A possible explanation for this observation is the lack of stabilizing salts and pH buffers in this lysis buffer, which created a hypotonic environment that led to the excessive lysis of both free-floating nuclei and large cell clumps. This would explain why most of the nuclei released were from these large cell clumps, and that these large cell clumps likely didn't filter into the final nuclei suspensions, leading to the significant reductions in nuclei yields.

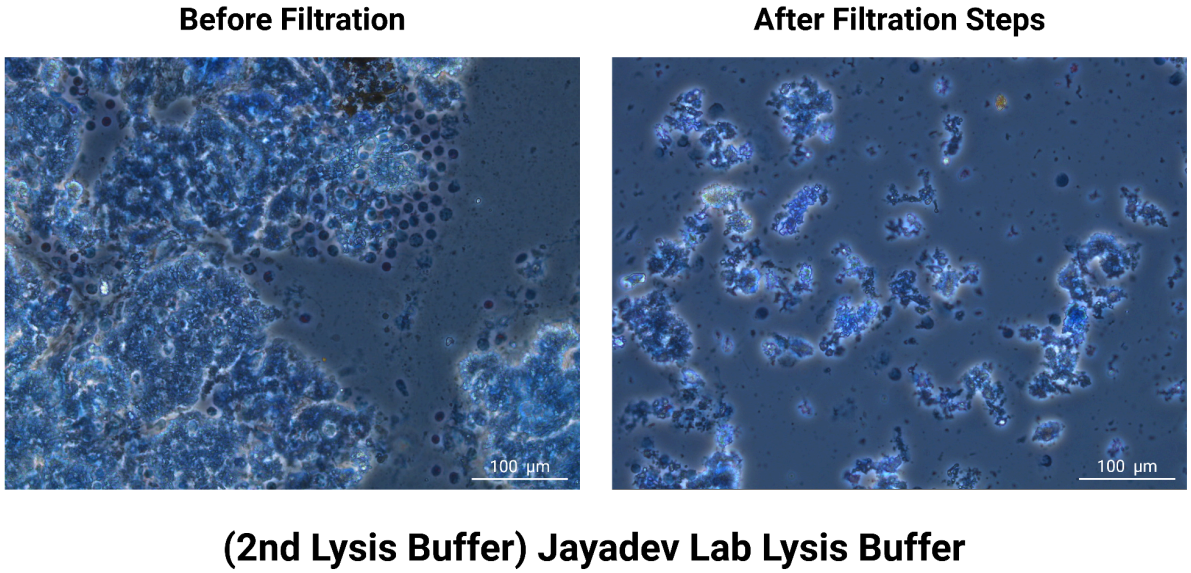


Fig 17. Lysis and filtration of brain tissue samples using the Jayadev lab lysis and nuclei wash buffers. Suspensions were filtered through both the 70 µm and 40 µm cell strainers. Scale bar is 100 µm.

Unlike the buffers used in the 2022 Bomsztyk liver single nuclei isolation protocol, sample suspensions using the Jayadev lab lysis and nuclei wash buffers were able to successfully pass through both the 70 µm and 40 µm cell strainers, likely due to the BSA content in the lysis and nuclei wash buffers limiting the aggregation of nuclei. However, the lack of free-floating nuclei before filtration and the significant reductions in final nuclei yields after filtration prompted us to conclude that this lysis buffer was not fully optimized. This lysis buffer was therefore omitted from the second and third preliminary experiments, as well as from the finalized single-nuclei isolation protocol.

When the optimized lysis buffer and the Jayadev lab nuclei wash buffer were tested against the first preliminary experimental protocol, there was a noticeable increase in free-floating nuclei and fewer cellular and nuclei aggregates. Although the nuclei yield after filtration was noticeably lower, intact, free-floating nuclei were still present in the final suspension. Given that the nuclei suspensions using the optimized lysis buffer were able to successfully filter through both the 70 µm and 40 µm cell strainers, and a significant number of free-floating, intact nuclei were present in the final nuclei suspensions, this lysis buffer and the Jayadev lab nuclei wash buffer were considered to be the most optimized buffers and were the only buffers incorporated in the second and third preliminary experimental protocols as well as in the finalized single-nuclei isolation protocol.

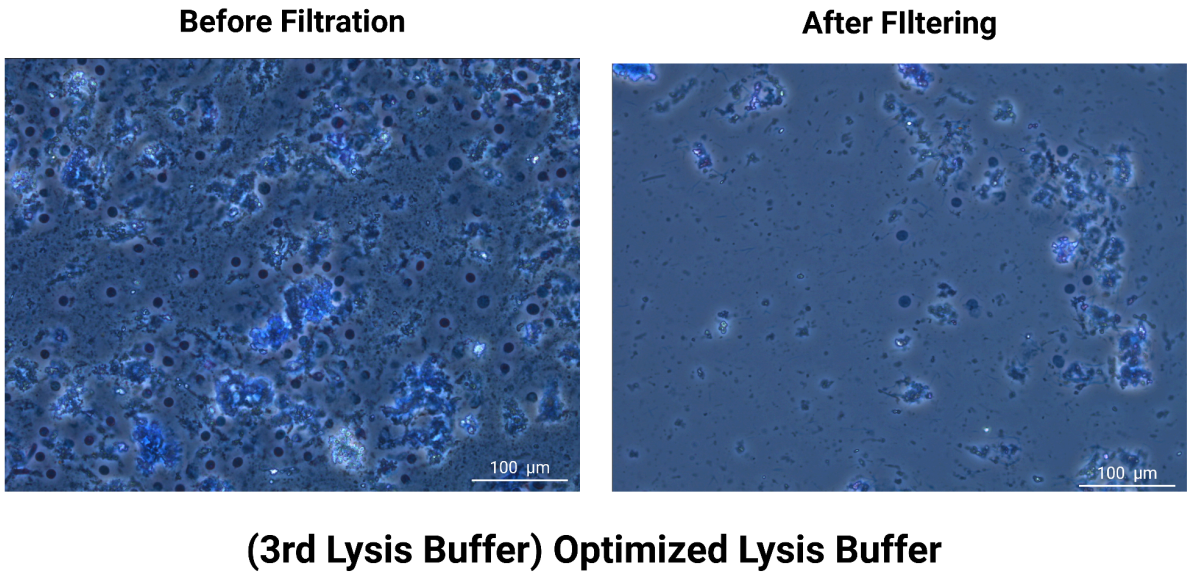


Fig 18. Lysis and filtration of brain tissue samples using the optimized lysis buffer and the Jayadev nuclei wash buffer. Suspensions were filtered through both the 70 µm and 40 µm cell strainers. Scale bar is 100 µm.

**Preliminary Experiment 2:** *Optimizing the Number of Tissue Cores for each Sample*

When the two-tissue core sample was homogenized in the PIXUL, very few nuclei were visible, and when the sample was filtered through the 200 μm cell strainer, the observed nuclei yield was even lower. When the four-tissue core sample was homogenized in the PIXUL, the nuclei yield after homogenization was slightly higher than the two-tissue core samples. Similarly to the two-tissue core sample, when the four-tissue core sample was filtered through the 200 μm cell strainer, the observed nuclei yield was lower but still higher than the two-tissue core sample after filtration. When the six-tissue core sample was homogenized in the PIXUL, the observed nuclei yield was higher than the four-tissue core sample before filtration. When the six-tissue core sample was filtered through the 200 μm cell strainer, the overall observed nuclei yield was lower but still higher than the four-tissue core sample after filtration. When the eight-tissue core sample was homogenized in the PIXUL, the observed nuclei yield was higher than the six-tissue core sample, and when the eight-tissue core sample was filtered through the 200 μm cell strainer, the observed nuclei yield was lower but still higher than the six-tissue core sample after filtration. Finally, when the 10-tissue core sample was homogenized in the PIXUL, the overall observed nuclei yield was the highest out of all the samples processed, and although the overall yield did decreased after filtration through the 200 μm cell strainer, the 10-tissue core sample still had the highest observed nuclei yield out of all of the samples homogenized. Based on this experiment, it was concluded that increasing the number of brain tissue cores was generally correlated with a higher nuclei yield after lysis and filtration. It's important to note that all samples still had cell and nuclei aggregates present right after homogenization and after filtration. Based on these results, the 10-tissue core sample was regarded as the most optimal number of tissue cores to add to a sample and was therefore the number of tissue cores used for each sample in the third preliminary experiment, as well as in the finalized brain single-nuclei isolation protocol.

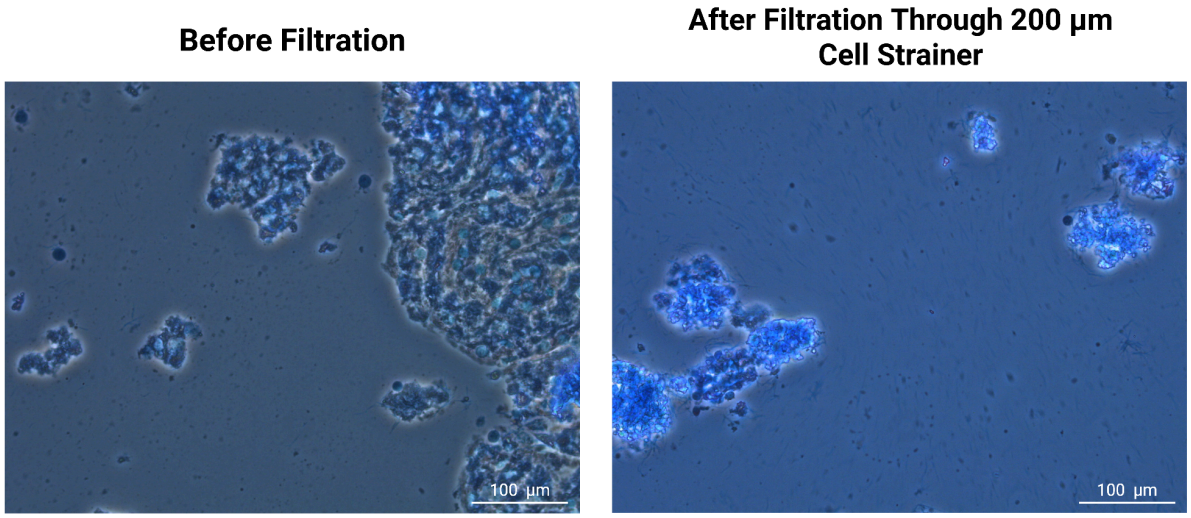


Fig 19. Lysis and filtration of a brain tissue sample with 2 cores: very few intact nuclei were observed right after lysis. Fewer nuclei were observed after the nuclei suspension was filtered through a 200 µm cell strainer. Scale bar is 100 µm.

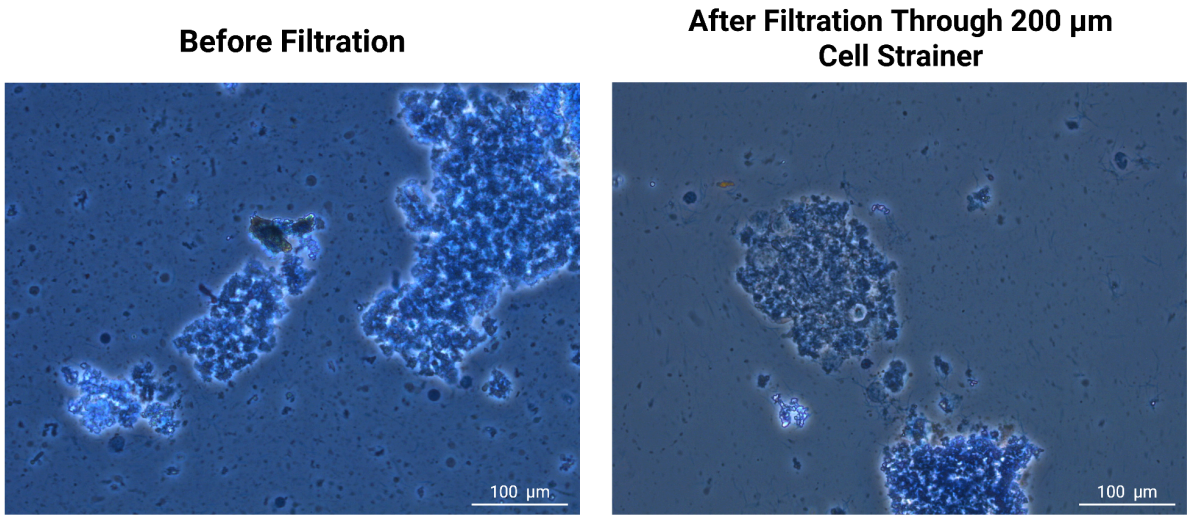


Fig 20. Lysis and filtration of a brain tissue sample with 4 cores: compared to the 2-core sample, more nuclei were observed right after lysis and filtration through a 200 µm cell strainer, however, the nuclei yield was still very low. Scale bar is 100 µm.

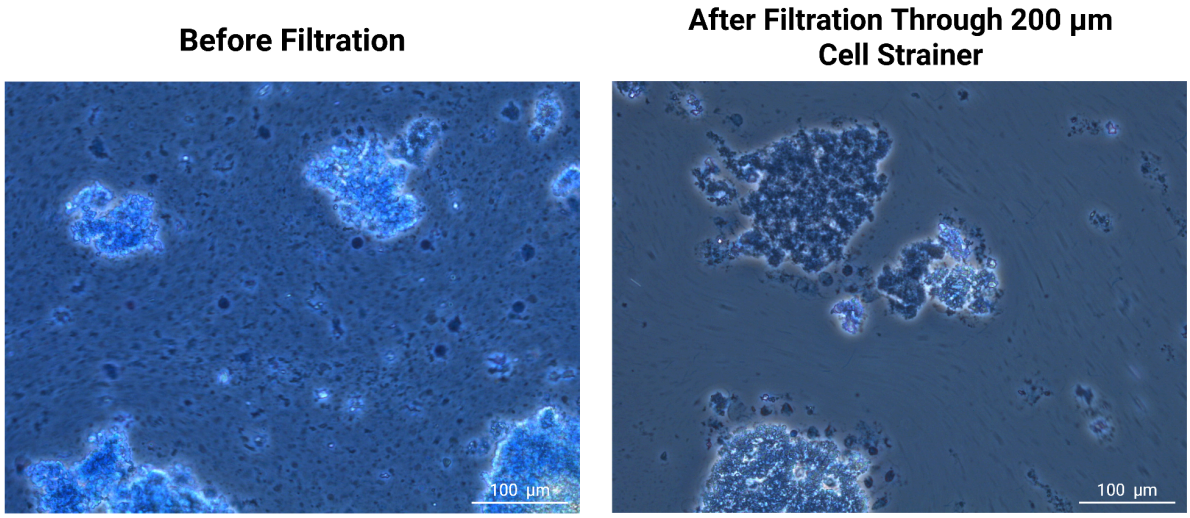


Fig 21. Lysis and filtration of a brain tissue sample with 6 cores: compared to the 4-core sample, more nuclei were observed right after lysis and filtration through a 200 µm cell strainer, however, the nuclei yield was still very low. Scale bar is 100 µm.

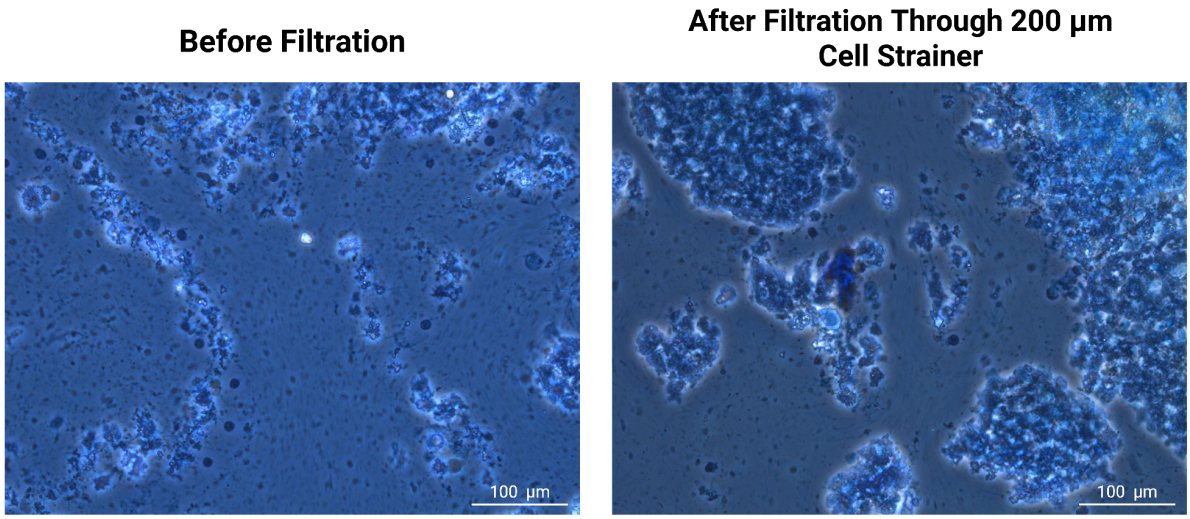


Fig 22. Lysis and filtration of a brain tissue sample with 8 cores: compared to the 6-core sample, the nuclei yield right after lysis and filtration through a 200 µm cell strainer was much higher. Scale bar is 100 µm.

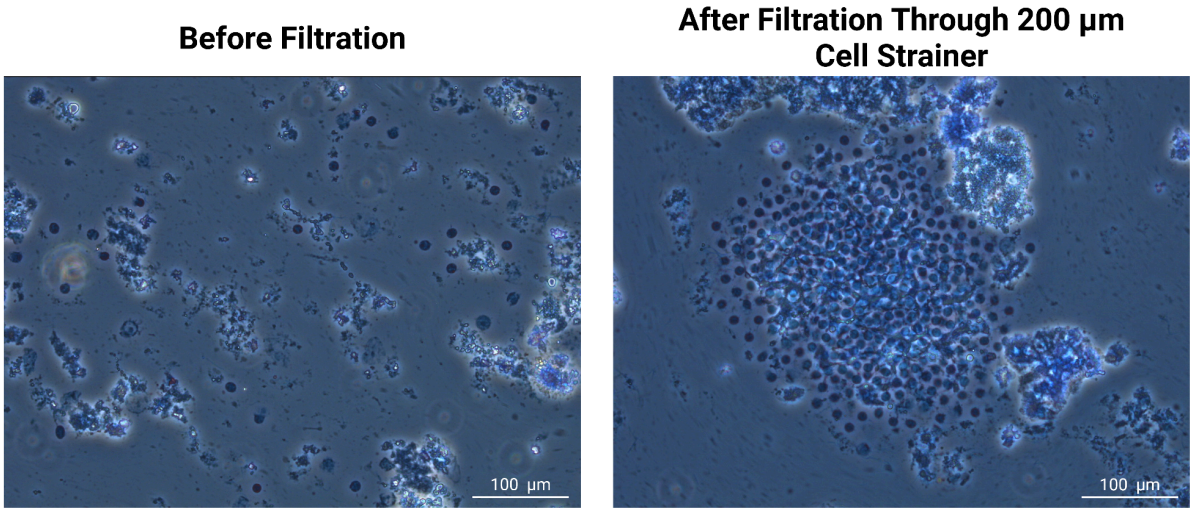


Fig 23. Lysis and filtration of a brain tissue sample with 10 cores: compared to the other samples, the 10-core sample yielded the most nuclei right after lysis and filtration through a 200 µm cell strainer. Scale bar is 100 µm.

**Preliminary Experiment 3:** *Optimizing the PIXUL Settings*

Immediately after the 10-tissue core sample was homogenized in the PIXUL for 30 seconds, there was a considerable amount of cell aggregation and very few nuclei present. Right after these samples were filtered through the 70 µm cell strainer, the observed nuclei yield was even lower. When the 10-tissue core sample was homogenized in the PIXUL for 1 minute, there was a significant increase in nuclei yield before filtration and less cell aggregation. Although the observed nuclei yield after filtration through the 70 µm cell strainer was noticeably lower, the final nuclei yield was still higher than the 30-second homogenization duration. When the 10-tissue core sample was homogenized in the PIXUL for 2 minutes, the observed nuclei yield before filtration was noticeably the highest out of all samples processed, and although the yield was significantly lower right after filtration, this 2-minute duration sample still had the largest observed nuclei yield out of all of the samples.

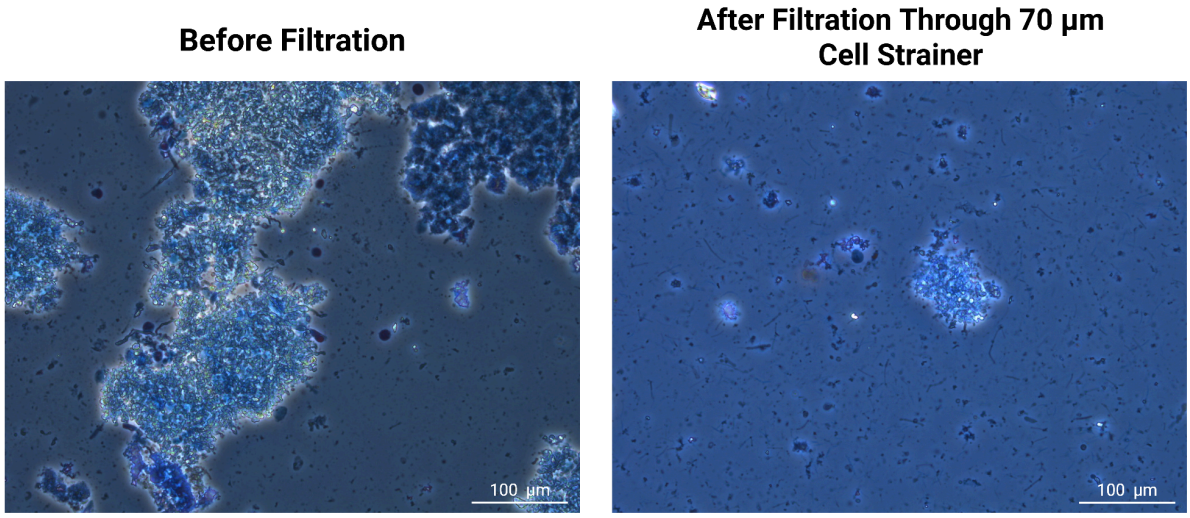


Fig 24. PIXUL homogenization duration of 30 seconds: before and after filtration of the nuclei suspension. Before filtration, few nuclei were observed, and they were primarily near large cell clumps. After filtration through a 70 µm cell strainer, fewer nuclei were observed. Scale bar is 100 µm.

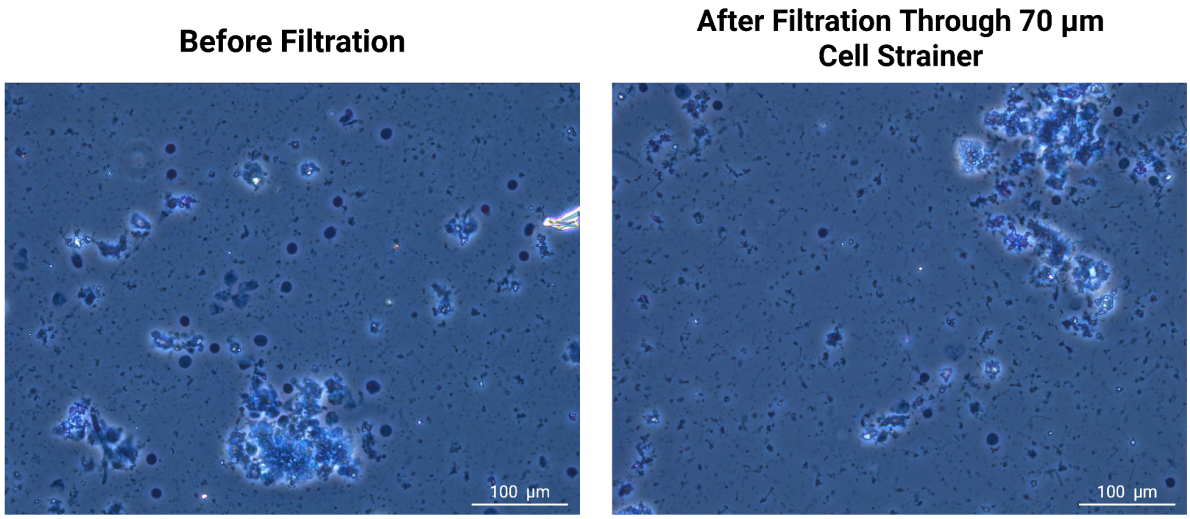


Fig 25. PIXUL homogenization duration of 1 minute: before and after filtration of the nuclei suspension. Free-floating nuclei were observed before filtration, and multiple nuclei were observed after filtration through a 70 µm cell strainer. Scale bar is 100 µm.

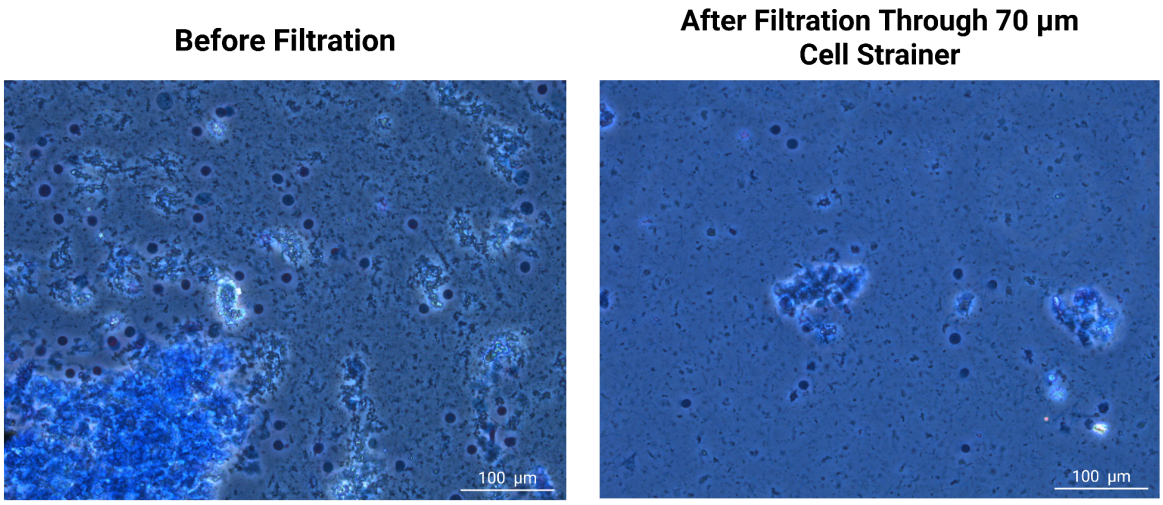


Fig 26. PIXUL homogenization duration of 2 minutes: before and after filtration of the nuclei suspension. Free-floating nuclei were observed before filtration, and multiple nuclei were observed after filtration through a 70 µm cell strainer. Scale bar is 100 µm.

In direct contrast, when the 10-tissue core sample was processed in the PIXUL for 4 minutes, the number of free-floating nuclei was noticeably fewer than the 2-minute duration sample. Additionally, there was significantly more nuclei aggregation, and when this sample was filtered through the 70 µm cell strainer, the nuclei yield was significantly lower and very comparable to the 30-second duration sample. When the 10-tissue core sample was homogenized in the PIXUL for 6 minutes, there was significant lysis of both cells and nuclei, thus yielding the lowest observable nuclei yield out of all samples processed. As expected, when this sample was filtered through the 70 µm cell strainer, the observed nuclei yield was the lowest out of all samples. Based on these results, the 2-minute homogenization duration was deemed to be the most optimal homogenization duration to maximize the number of nuclei released from the brain cells. This 2-minute homogenization duration was therefore used in the finalized brain single-nuclei isolation protocol.

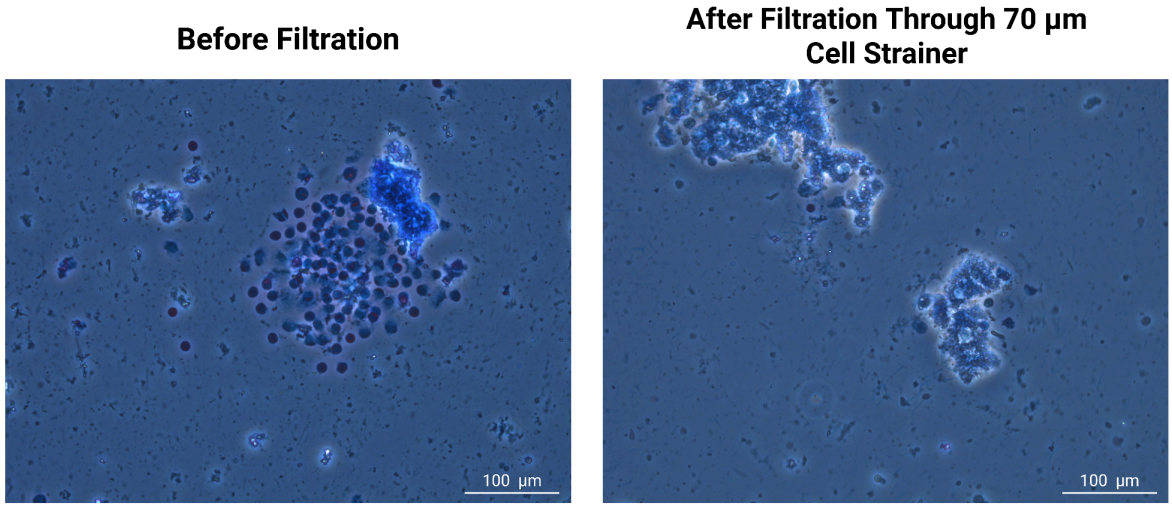


Fig 27. PIXUL homogenization duration of 4 minutes: before and after filtration of the nuclei suspension. Nuclei were mainly observed in clumps before filtration, and very few nuclei were observed after filtration through a 70 µm cell strainer. Scale bar is 100 µm.

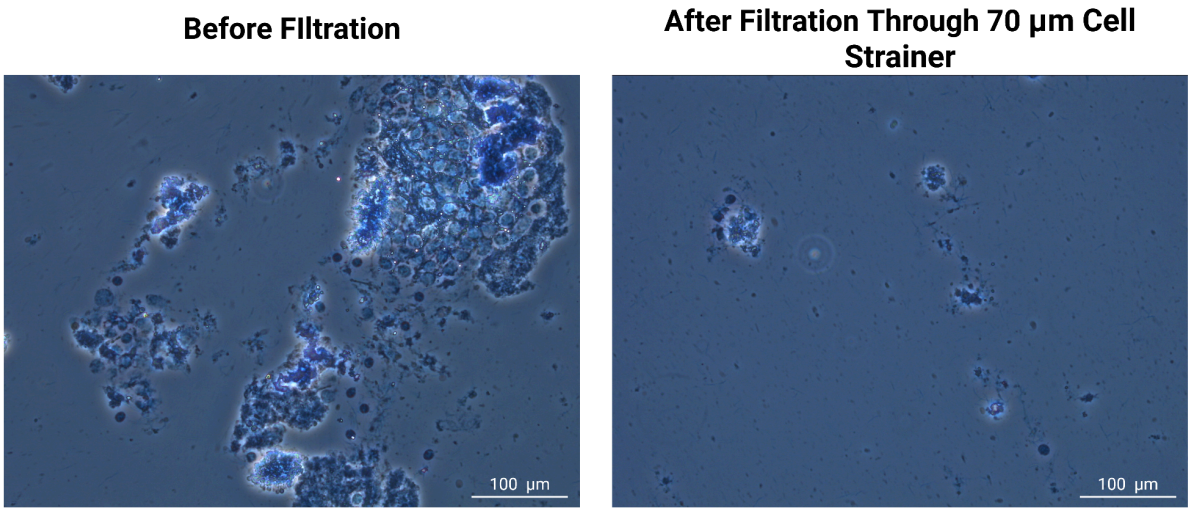


Fig 28. PIXUL homogenization duration of 6 minutes: before and after filtration of the nuclei suspension. Significant lysis of both cells and nuclei was present, and very few nuclei were observed after filtration through a 70 µm cell strainer. Scale bar is 100 µm.

**<u>Finalized Protocol</u>: PIXUL High-Throughput Brain Single Nuclei Isolation**

*Trypan Blue Nuclei Staining Results - Assessing Lysis Efficiency and Nuclei Integrity*

Three separate trials were conducted using the same finalized, high-throughput brain single nuclei isolation protocol developed in this paper, which essentially yielded 6 identical sample replicates. Right after the samples were homogenized using the PIXUL, they were stained with trypan blue dye and examined under the microscope to assess the lysis efficiency. Samples 3, 4, and 6 yielded the highest number of observable free-floating nuclei, while sample 1 yielded the lowest. It's important to emphasize that all samples contained both free-floating and aggregated nuclei, and although excessive cell debris and lysis of both cells and nuclei were observed in all samples right after tissue homogenization, samples 2 and 5 noticeably had the most lysed cellular and nuclei debris right after sample homogenization using the PIXUL.

After all of the samples were filtered through the 70 µm and 40 µm cell strainers, they underwent a series of wash steps to remove any remaining cell and nuclei debris and to preserve the remaining, intact nuclei. Afterwards, these samples were stained with trypan blue dye and observed under the microscope. As expected, samples 3, 4, and 6 contained the most free-floating nuclei, however, a considerable amount of cellular debris and lysed nuclei remained in all samples. The excessive cellular and nuclei debris observed in samples 2 and 5 right after tissue homogenization was significantly reduced after the wash steps were completed.

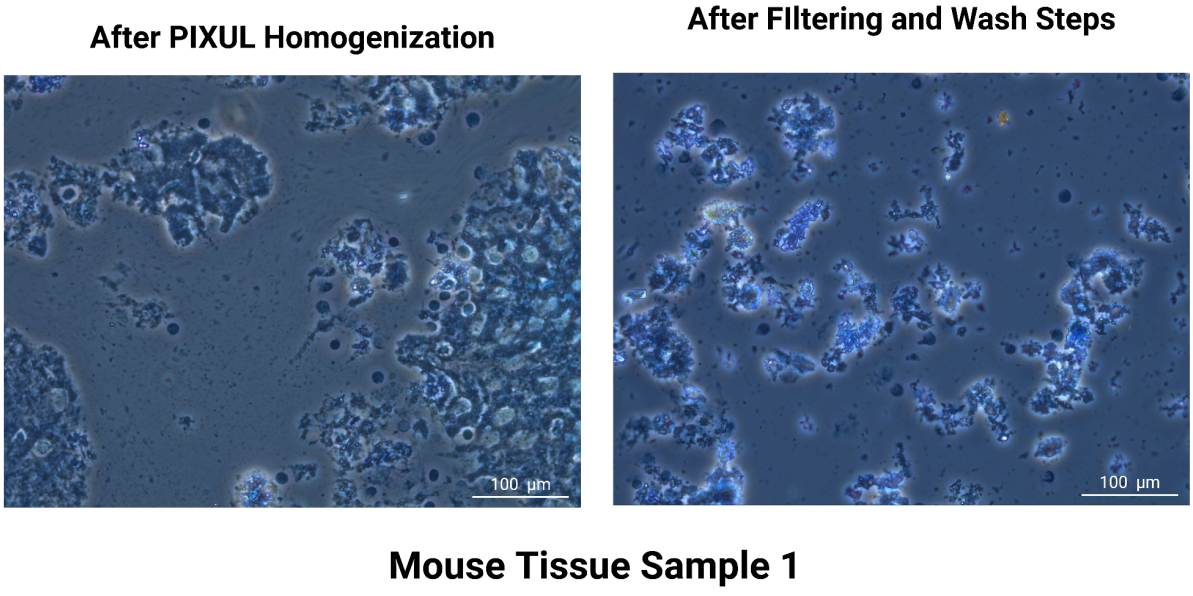


Fig 29. Trypan blue staining of replicate 1 was performed right after tissue homogenization and after all of the wash steps were completed. Intact free-floating nuclei were observed after tissue homogenization, and after the wash steps were performed. Replicate 1 noticeably had the fewest observed nuclei. Cellular debris and lysed cells, and nuclei were observed during both stages of the protocol.

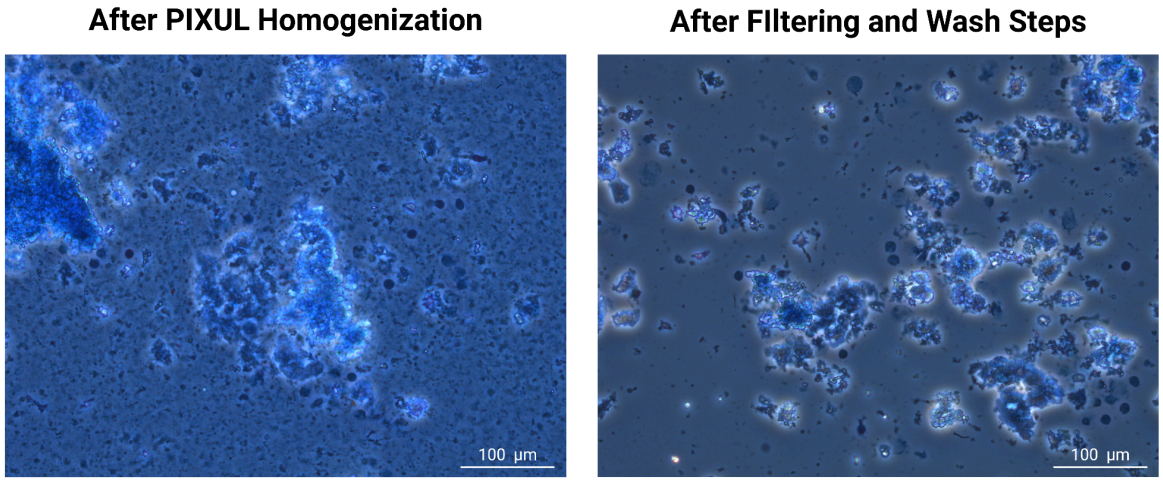


## Mouse Tissue Sample 2

Fig 30. Trypan blue staining of replicate 2 was performed right after tissue homogenization and after all of the wash steps were completed. Intact free-floating nuclei were observed after tissue homogenization, and after the wash steps were performed; however, significant cellular and nuclei debris were observed right after tissue homogenization. After the wash steps were completed, the cellular and nuclei debris were reduced, and replicate 2 had more observed nuclei than replicate 1.

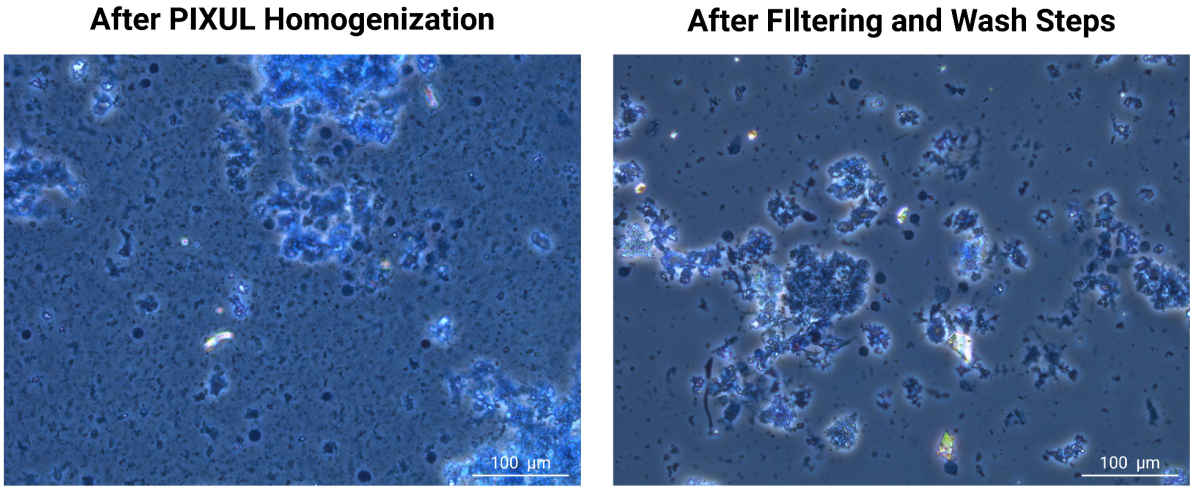


## Mouse Tissue Sample 3

Fig 31. Trypan blue staining of replicate 3 was performed right after tissue homogenization and after all of the wash steps were completed. Replicate 3, as well as replicates 4 and 6, had the most observed intact free-floating nuclei after tissue homogenization and after the wash steps were performed. Cellular and nuclei debris were observed right after tissue homogenization and after the wash steps were completed.

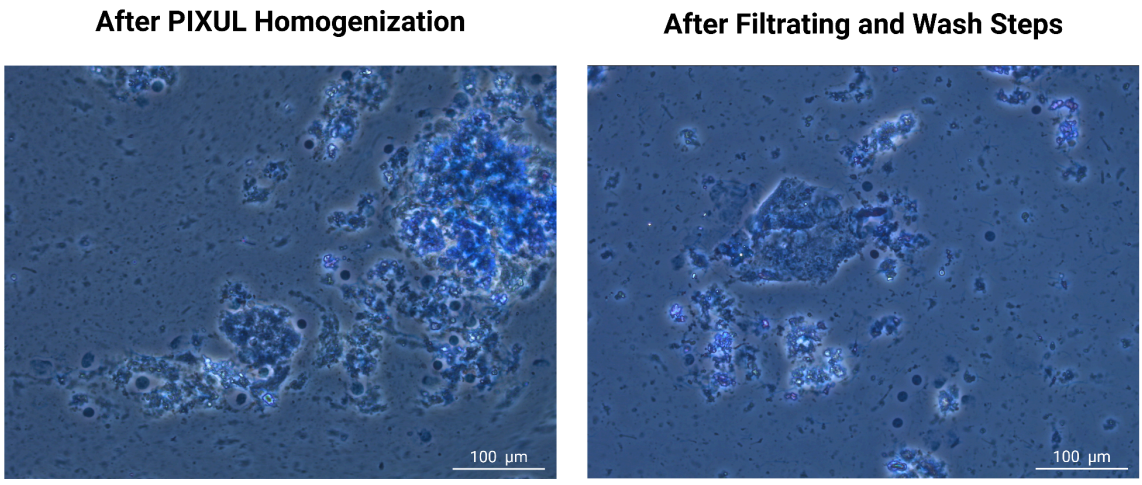


Fig 32. Trypan blue staining of replicate 4 was performed right after tissue homogenization and after all of the wash steps were completed. Replicate 4, as well as replicates 3 and 6, had the most observed intact free-floating nuclei after tissue homogenization and after the wash steps were performed. Cellular and nuclei debris were observed right after tissue homogenization and after the wash steps were completed.

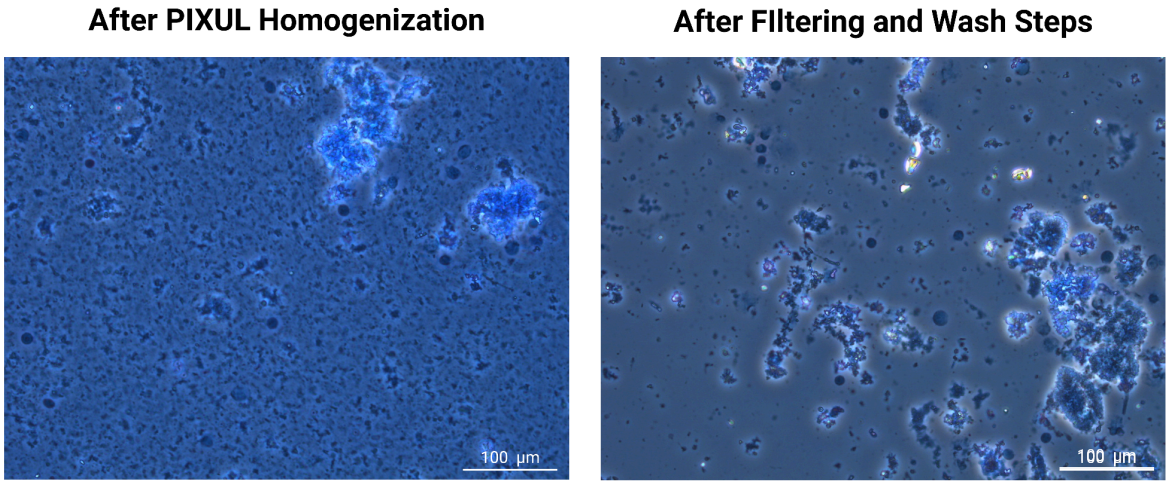


Fig 33. Trypan blue staining of replicate 5 was performed right after tissue homogenization and after all of the wash steps were completed. Intact free-floating nuclei were observed after tissue homogenization, and after the wash steps were performed; however, similarly to replicate 2, significant cellular and nuclei debris were observed right after tissue homogenization. After the wash steps were completed, the cellular and nuclei debris were reduced, and replicate 5 had more observed nuclei than replicate 1.

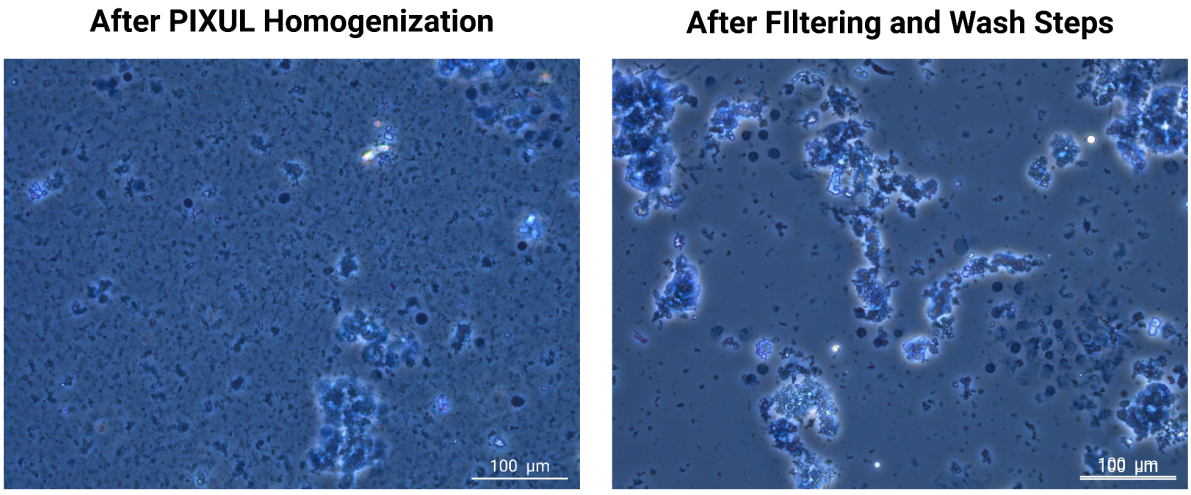


Fig 34. Trypan blue staining of replicate 6 was performed right after tissue homogenization and after all of the wash steps were completed. Replicate 6, as well as replicates 3 and 4, had the most observed intact free-floating nuclei after tissue homogenization and after the wash steps were performed. Cellular and nuclei debris were observed right after tissue homogenization and after the wash steps were completed.

*Hemocytometer Results*

The final nuclei concentrations of all six replicates were calculated using a hemocytometer, a manual cell counter. The final calculated nuclei concentrations for samples 1, 2, 3, 4, 5, and 6, was $9.35 \times 10^5$ nuclei/mL, $1.67 \times 10^6$ nuclei/mL, $2.01 \times 10^6$ nuclei/mL, $1.83 \times 10^6$ nuclei/mL, $1.48 \times 10^6$ nuclei/mL, and $1.95 \times 10^6$ nuclei/mL, respectively. The average nuclei concentration was calculated to be $1.65 \times 10^6$ nuclei/mL, and the standard deviation was calculated to be $3.56 \times 10^5$ nuclei/mL.

| Replicate Name | Final Calculated Nuclei Concentration (nuclei/mL) |
|---|---|
| Sample 1 | $9.35 \times 10^5$ nuclei/mL |
| Sample 2 | $1.67 \times 10^6$ nuclei/mL |
| Sample 3 | $2.01 \times 10^6$ nuclei/mL |
| Sample 4 | $1.83 \times 10^6$ nuclei/mL |
| Sample 5 | $1.48 \times 10^6$ nuclei/mL |
| Sample 6 | $1.95 \times 10^6$ nuclei/mL |
| Total Average | $1.65 \times 10^6$ nuclei/mL |
| Standard Deviation | $3.56 \times 10^5$ nuclei/mL |

Table 6. Final calculated nuclei concentration of all 6 replicates in units of nuclei/mL. The average nuclei concentration and its standard deviation were calculated.

Given that the nuclei outputs for manual isolation protocols, nuclei isolation kits, and semi-automated isolation protocols are $7.0 \times 10^5$ - $1.2 \times 10^6$ nuclei/mL, $7.0 \times 10^5$ - $1.04 \times 10^8$ nuclei/mL, and $9.09 \times 10^5$ - $1.18 \times 10^7$ nuclei/mL, respectively, the averaged calculated nuclei concentration of $1.65 \times 10^6$ nuclei/mL is very comparable to the nuclei output of these other isolation methods.

| Protocol Type | Final Calculated Nuclei Concentration (nuclei/mL) |
|---|---|
| Manual Single-Nuclei Isolation | $7.0 \times 10^5$ - $1.2 \times 10^6$ nuclei/mL |
| Nuclei Isolation Kits | $7.0 \times 10^5$ - $1.04 \times 10^8$ nuclei/mL |
| Semi-automated Single-Nuclei Isolation | $9.09 \times 10^5$ - $1.18 \times 10^7$ nuclei/mL |
| Finalized PIXUL Single-Nuclei Isolation | $1.65 \times 10^6$ nuclei/mL |

Table 7. Comparing the final, average nuclei concentration achieved by the finalized PIXUL brain single-nuclei isolation protocol to the nuclei concentration outputs from other existing single-nuclei isolation methods

# Discussion:

*Trypan Blue Nuclei Staining - Assessing Lysis Efficiency and Nuclei Integrity*

Although free-floating, intact nuclei were observed in all six replicates after tissue homogenization and after the filtering and wash steps were completed, there were some noticeable differences in tissue homogenization and observed nuclei yield between the replicates. Samples 3, 4, and 6 had noticeably the largest intact observed nuclei yield right after the tissue homogenization step and the filtering and wash steps. Compared to the other samples, sample 1 had the least observed nuclei yield right after the tissue homogenization step and the filtering and wash steps, while samples 2 and 5 had a larger nuclei yield than sample 1 but not as large as samples 3, 4, and 6.

In addition to this observation, samples 2 and 5 noticeably had the most lysed cellular and nuclei debris right after tissue homogenization, but this debris was visibly reduced after the wash steps. A significant amount of cellular and nuclei debris was present in all samples, even after the wash steps were performed. These resulting discrepancies in tissue homogenization and cell lysis could be explained by several factors. One potential factor is that all samples were still suspended in the lysis buffer when they were stained with trypan blue and observed under the microscope, which could have resulted in additional lysing of cells and intact nuclei. It's also important to acknowledge that the lysis of cells and release of nuclei was not completely uniform throughout any nuclei suspension. For all samples, right after tissue homogenization, some regions of the nuclei suspension contained multiple free-floating nuclei, while other regions had multiple cell and nuclei aggregate clumps, even after the filtration and wash steps. Some of these cellular and nuclei clumps likely failed to filter through and remain in the nuclei suspension after

the wash steps were performed, which would explain the lower intact nuclei yield for all replicates. Lastly, the mouse brain is small, and the difference in the samples might reflect different regions of the brain. These studies need to be repeated in frozen human brains, where there would be better control for sampling specific brain regions. In future experiments, the lysis buffer from each sample would likely need to be aspirated and replaced with the nuclei wash buffer immediately after the homogenization step to prevent extended lysing and production of cellular and nuclei debris when the lysis efficiency for each sample is assessed with trypan blue dye.

Despite optimizing the PIXUL settings for this specific isolation protocol through the preliminary experiments, excessive cellular and nuclei debris were present right before filtering, which was likely due to the excessive lysis of both nuclei and cells during the tissue homogenization process. The PIXUL settings will likely need to be further optimized and tested against mouse and human brain tissue samples. Additional follow-up experiments can either focus on further reducing the Pulse or Time Duration settings, as decreasing the pulse setting or the time duration could reduce the amount of ultrasound energy focused into each well and prevent excessive cellular and nuclei lysis. It may also be worth experimenting with lower burst rates to further minimize the amount of focused ultrasound energy into each well. Additionally, the presence of excessive cellular and nuclei debris after the wash steps is a significant concern for those who want to use the nuclei for gene sequencing applications. This debris will likely make it difficult to target the intact nuclei for sequencing, and there's a high likelihood that the DNA contamination from the lysed cells could interfere with the accuracy of snRNA-seq. Although some of this debris is likely extracellular DNA released from the lysed cells, some of this debris is also myelin debris, as the brain contains a significant amount of neuronal tissue. Additional wash steps could help remove this myelin debris; however, myelin can also be removed using sucrose gradients and myelin removal beads. [25, 26]. In addition to decreasing the accuracy of gene sequencing applications such as snRNA-seq, extracellular DNA can lead to the aggregation of both cells and nuclei. This could explain the persistent number of cellular and nuclei aggregations observed in all six sample replicates. A potential method to minimize this extracellular DNA would be to incorporate enzymes, such as DNase I, into the isolation protocol to digest this extracellular DNA. [Ling]

*Hemocytometer*

Although the final average nuclei concentration was $1.65 \times 10^6$ nuclei/mL and samples 1, 2, 3, 4, 5, and 6 had a final nuclei concentration of $9.35 \times 10^5$ nuclei/mL, $1.67 \times 10^6$ nuclei/mL, $2.01 \times 10^6$ nuclei/mL, $1.83 \times 10^6$ nuclei/mL, $1.48 \times 10^6$ nuclei/mL, and $1.95 \times 10^6$ nuclei/mL, which are all comparable nuclei yields found in other manual and automated nuclei isolation protocols, the standard deviation value of $3.56 \times 10^5$ nuclei/mL is substantially large and likely suggests that the final nuclei concentration outputs from this protocol are highly variable and inconsistent. In this case, future experimentation is required to determine whether these results are truly inconsistent or not, however, based on the trypan blue staining images obtained after the homogenization step and after the wash steps, it's likely that the lysis and homogenization of samples are not uniform or consistent enough to generate reliable, reproducible results. It's also important to consider that discrepancies in nuclei concentration calculations could likely be due to user error when observing the nuclei loaded into the hemocytometer. Using a hemocytometer

to count nuclei is prone to subjective bias, and many users may have trouble distinguishing between free nuclei and debris.

Although automated cell counters are not suitable for counting nuclei derived from brain tissues due to the excessive cellular debris produced from these tissues, it's important to recognize that using a hemocytometer to calculate nuclei concentrations is not an optimal cell counting method for high-throughput applications, as it is time-consuming and can lead to significant eye strain and fatigue. Given that this protocol is designed to generate nuclei at a high-throughput rate, it's worth exploring tools such as flow cytometry to count nuclei more accurately and at an efficient rate. Additionally, future experiments are needed to evaluate the feasibility of processing more than two samples simultaneously to determine whether this protocol can efficiently and consistently yield a high number of nuclei from multiple samples. The time it takes to complete this protocol with two samples is around 2.5 hours, which is not nearly as efficient as the 6 minutes that The Singulator 100 by S2 genomics can achieve when processing two samples. [20] The inefficiency of this finalized isolation protocol is likely rooted in the constant transferring of samples to LoBind tubes. Given that the temperature-modulated centrifuge used in the Bomsztyk lab only uses micro-tubes, the only feasible way to centrifuge samples at 4℃ was to transfer these samples from the 96-well plate to LoBind tubes. To increase the efficiency of this protocol, it's worth exploring methods to limit the repeated transfer of samples. For this protocol, it may be worth investing in a temperature-modulated 96-well plate centrifuge for further protocol optimization.

## Experimental Challenges:

There were a number of challenges during the development of this high-throughput brain single-nuclei isolation protocol. Notably, optimizing the lysis buffers took approximately 3 months to complete, as most of the time was spent experimenting with the lysis buffer used in the Jayadev lab. There were many samples where this lysis buffer was able to produce a significantly high yield of nuclei; however, despite using the same number of brain tissue cores and PIXUL settings, there were many instances where results varied and produced a significantly lower nuclei yield. This variability in the lysing of brain tissue samples prompted us to shift our focus to developing a more optimized lysis buffer. The final optimized lysis buffer produced more consistent nuclei yields and was therefore the only lysis buffer integrated in the final protocol. Though it is important to note that the current protocol still produces variations in tissue homogenization and cell lysing, which need to be further optimized.

Additionally, optimizing the PIXUL settings took significant effort and time. For nearly 2 months, most of the experiments were focused on optimizing the PIXUL settings, and initially, the 4-minute tissue homogenization duration was thought to produce the highest nuclei yield. However, despite keeping experimental conditions identical, this homogenization duration often produced variable observed nuclei yields. Despite producing some of the largest observed nuclei yields in the lab, this homogenization duration was not chosen as the most optimized PIXUL setting for the final protocol, given the nuclei yield inconsistencies. The 2-minute duration was able to achieve more consistent nuclei yields compared to the 4-minute duration and was therefore preferred over the 4-minute duration.

The most prominent challenge that occurred during the development of this protocol was the persistent presence of both cellular and nuclei aggregates in all samples, despite the optimization of the lysis buffer and the PIXUL homogenization settings. The most probable explanation for this is the notion that lysed brain cells often release extracellular DNA that significantly contributes to the aggregation of both cells and nuclei. For future experiments, it's worth exploring enzymes, such as DNase I, that can digest this extracellular DNA to reduce both DNA contamination and cellular and nuclei aggregation in final nuclei suspensions.

# Conclusion:

Although this novel, high-throughput protocol was able to achieve final nuclei concentrations that were very comparable to nuclei concentration outputs from manual isolation protocols, nuclei isolation kits, and semi-automated single nuclei isolation protocols, a significant amount of cellular and nuclei debris and aggregation was present in all replicates, even when the samples were filtered and underwent multiple wash steps. The excessive cellular and nuclei debris after homogenization was likely due to extended sample suspension in the lysis buffer and unoptimized PIXUL parameters for tissue homogenization. Additionally, some of the cellular and nuclei debris present after filtration and the wash steps is likely myelin debris, which needs to be removed following filtration and the wash steps. To reduce the amount of excess cellular and nuclei debris after homogenization and filtration, it's important to alter the protocol so that the lysis buffer is immediately aspirated and replaced with a nuclei wash buffer right after homogenization, and it's important to consider adding a myelin removal step either by using sucrose gradients or myelin removal beads.

The presence of cellular and nuclei aggregation is likely due to the presence of extracellular DNA, which can enhance the aggregation of both cells and nuclei. Additionally, this extracellular debris can interfere with the accuracy of gene sequencing applications, such as snRNA-seq. To reduce the amount of extracellular DNA in the nuclei suspensions, it's worth exploring the integration of enzymes, such as DNase I, into the final protocol to digest these extracellular DNA contaminants.

Finally, this protocol takes approximately 2.5 hours to completely process two brain tissue samples, making it significantly less efficient than other single-nuclei isolation protocols. Future experiments should focus on further optimizing the PIXUL settings and limiting the number of repeated sample transfers between the 96-well plate and LoBind tubes. Investing in a temperature-modulated 96-well plate centrifuge could be a solution to reduce the number of sample transfers in this protocol and improve the overall protocol efficiency. These experiments will help improve the protocol and generate more reliable and reproducible nuclei yields that are suitable for high-throughput gene sequencing applications.

# Acknowledgments:

A special thank you to Dr. Karol Bomsztyk and Daniel Mar, who were instrumental in making this project possible. Without their guidance and assistance, this project wouldn't have successfully come to fruition.

- Dr. Karol Bomsztyl – PI and primary advisor
- Dr. Suman Jayadev – Committee advisor
    - Lexi Sotelo – Jayadev Lab member
    - Aquene Reid – Jayadev Lab member
- Dr. Ying Zheng – Committee advisor
- Daniel Mar - Lab technician, lab procedure training

# References:

1. Alzheimer's disease fact sheet | National Institute on Aging. (n.d.). https://www.nia.nih.gov/health/alzheimers-and-dementia/alzheimers-disease-fact-sheet
2. What happens to the brain in alzheimer's disease? | National Institute on Aging. (n.d.). https://www.nia.nih.gov/health/alzheimers-causes-and-risk-factors/what-happens-brain-alzheimers-disease
3. *Alzheimer's disease facts and figures*. Alzheimer's Association. (n.d.). https://www.alz.org/alzheimers-dementia/facts-figures
4. Hayes M. T. (2019). Parkinson's Disease and Parkinsonism. *The American journal of medicine*, *132*(7), 802–807. https://doi.org/10.1016/j.amjmed.2019.03.001
5. World Health Organization. (n.d.-a). *Parkinson disease*. World Health Organization. https://www.who.int/news-room/fact-sheets/detail/parkinson-disease
6. *What is parkinson's?* Parkinson's Foundation. (n.d.). https://www.parkinson.org/understanding-parkinsons/what-is-parkinsons
7. Wirsching, H. G., Galanis, E., & Weller, M. (2016). Glioblastoma. *Handbook of clinical neurology*, *134*, 381–397. https://doi.org/10.1016/B978-0-12-802997-8.00023-2
8. Thakkar, J. P., Dolecek, T. A., Horbinski, C., Ostrom, Q. T., Lightner, D. D., Barnholtz-Sloan, J. S., & Villano, J. L. (2014). Epidemiologic and molecular prognostic review of glioblastoma. *Cancer epidemiology, biomarkers & prevention : a publication of the American Association for Cancer Research, cosponsored by the American Society of Preventive Oncology*, *23*(10), 1985–1996. https://doi.org/10.1158/1055-9965.EPI-14-0275
9. Tamimi, A. F., & Juweid, M. (2017). Epidemiology and Outcome of Glioblastoma. In S. De Vleeschouwer (Ed.), *Glioblastoma*. Codon Publications.
10. Caglar, H. O., & Duzgun, Z. (2023). Identification of upregulated genes in glioblastoma and glioblastoma cancer stem cells using bioinformatics analysis. *Gene*, *848*, 146895. https://doi.org/10.1016/j.gene.2022.146895
11. Mathys, H., Peng, Z., Boix, C. A., Victor, M. B., Leary, N., Babu, S., Abdelhady, G., Jiang, X., Ng, A. P., Ghafari, K., Kunisky, A. K., Mantero, J., Galani, K., Lohia, V. N., Fortier, G. E., Lotfi, Y., Ivey, J., Brown, H. P., Patel, P. R., Chakraborty, N., … Tsai, L. H. (2023). Single-cell atlas reveals correlates of high cognitive function, dementia, and resilience to Alzheimer's disease pathology. *Cell*, *186*(20), 4365–4385.e27.

https://doi.org/10.1016/j.cell.2023.08.039
12. Martirosyan, A., Ansari, R., Pestana, F., Hebestreit, K., Gasparyan, H., Aleksanyan, R., Hnatova, S., Poovathingal, S., Marneffe, C., Thal, D. R., Kottick, A., Hanson-Smith, V. J., Guelfi, S., Plumbly, W., Belgard, T. G., Metzakopian, E., & Holt, M. G. (2024). Unravelling cell type-specific responses to Parkinson's Disease at single cell resolution. *Molecular neurodegeneration*, *19*(1), 7. https://doi.org/10.1186/s13024-023-00699-0
13. García-Vicente, L., Martínez-Fernández, M., Borja, M., Tran, V., Álvarez-Vázquez, A., Flores-Hernández, R., Ding, Y., González-Sánchez, R., Granados, A., McGeever, E., Kim, Y. J., Detweiler, A., Mekonen, H., Paul, S., Pisco, A. O., Neff, N. F., & Tabernero, A. (2025). Single-nucleus RNA sequencing reveals a preclinical model for the most common subtype of glioblastoma. *Communications biology*, *8*(1), 671. https://doi.org/10.1038/s42003-025-08092-x
14. Ernst, K. J., Okonechnikov, K., Bageritz, J., Perera, A. A., Mallm, J. P., Wittmann, A., Maaß, K. K., Leible, S., Boutros, M., Pfister, S. M., Zuckermann, M., & Jones, D. T. W. (2025). A simplified preparation method for single-nucleus RNA-sequencing using long-term frozen brain tumor tissues. *Scientific reports*, *15*(1), 12849. https://doi.org/10.1038/s41598-025-97053-9
15. *Isolation of nuclei for single cell RNA sequencing & tissues for single cell RNA sequencing*. 10x Genomics. (n.d.). https://www.10xgenomics.com/support/universal-three-prime-gene-expression/documentation/steps/sample-prep/isolation-of-nuclei-for-single-cell-rna-sequencing-and-tissues-for-single-cell-rna-sequencing
16. Ayhan, F., Douglas, C., Lega, B. C., & Konopka, G. (2021). Nuclei isolation from surgically resected human hippocampus. STAR protocols, 2(4), 100844. https://doi.org/10.1016/j.xpro.2021.100844
17. *Nuclei isolation kit product sheet*. 10x Genomics. (n.d.-b). https://www.10xgenomics.com/library/d6ec7f
18. *Single nuclei isolation*. Invent Biotechnologies Inc. (n.d.). https://inventbiotech.com/collections/single-nuclei-isolation?srsltid=AfmBOooLe5TC1bjb5sJESMgOTJuQuA-ZcQpQOqe1hl5onz5KPOSKNPl_
19. *gentleMACSTM Octo Dissociator with Heaters*. Miltenyi Biotec. (n.d.). https://www.miltenyibiotec.com/US-en/products/gentlemacs-octo-dissociator-with-heaters.html
20. *Singulator platform*. S2 Genomics. (2025, May 5). https://s2genomics.com/singulator-platform/
21. Bomsztyk, K., Mar, D., Wang, Y., Denisenko, O., Ware, C., Frazar, C. D., Blattler, A., Maxwell, A. D., MacConaghy, B. E., & Matula, T. J. (2019). PIXUL-ChIP: integrated high-throughput sample preparation and analytical platform for epigenetic studies. *Nucleic acids research*, *47*(12), e69. https://doi.org/10.1093/nar/gkz222
22. Mannheim V, Simenfalvi Z. Total Life Cycle of Polypropylene Products: Reducing Environmental Impacts in the Manufacturing Phase. Polymers (Basel). 2020 Aug 24;12(9):1901. doi: 10.3390/polym12091901. PMID: 32846916; PMCID: PMC7563104.
23. S. Schactler, K. Bomsztyk, “PIXUL: High-throughput Nuclei Isolation Protocol for Frozen Mouse Liver Samples”. University of Washington May 2022.
24. Bedwell, L., Mavrotas, M., Demchenko, N., Yaa, R. M., Willis, B., Demianova, Z., Syed, N., Whitwell, H. J., & Nott, A. (2024). FANS Unfixed: Isolation and Proteomic Analysis

of Mouse Cell Type-Specific Brain Nuclei. *Journal of proteome research*, *23*(9), 3847–3857. https://doi.org/10.1021/acs.jproteome.4c00161

25. *Myelin Removal Beads II, human, mouse, rat*. Miltenyi Biotec. (n.d.-b). https://www.miltenyibiotec.com/US-en/products/myelin-removal-beads-ii-human-mouse-rat.html#size=for-up-to-400-separations
26. Walker, H., & Frost, N. A. (2024). Protocol for the generation of single-nuclei RNA-seq libraries and quantification of heterogeneous cell types activated during social interaction. *STAR protocols*, *5*(4), 103395. https://doi.org/10.1016/j.xpro.2024.103395
27. Ling, G., & Waxman, D. J. (2013). Isolation of nuclei for use in genome-wide DNase hypersensitivity assays to probe chromatin structure. *Methods in molecular biology (Clifton, N.J.)*, *977*, 13–19. https://doi.org/10.1007/978-1-62703-284-1_2